The Risk of Exposure to Diagnostic Ultrasound in Postnatal Subjects

Nonthermal Mechanisms

Charles C. Church, PhD, Edwin L. Carstensen, PhD, Wesley L. Nyborg, PhD, Paul L. Carson, PhD, Leon A. Frizzell, PhD, Michael R. Bailey, PhD

This review examines the nonthermal physical mechanisms by which ultrasound can harm tissue in postnatal patients. First the physical nature of the more significant interactions between ultrasound and tissue is described, followed by an examination of the existing literature with particular emphasis on the pressure thresholds for potential adverse effects. The interaction of ultrasonic fields with tissue depends in a fundamental way on whether the tissue naturally contains undissolved gas under normal physiologic conditions. Examples of gas-containing tissues are lung and intestine. Considerable effort has been devoted to investigating the acoustic parameters relevant to the threshold and extent of lung hemorrhage. Thresholds as low as 0.4 MPa at 1 MHz have been reported. The situation for intestinal damage is similar, although the threshold appears to be somewhat higher. For other tissues, auditory stimulation or tactile perception may occur, if rarely, during exposure to diagnostic ultrasound; ultrasound at similar or lower intensities is used therapeutically to accelerate the healing of bone fractures. At the exposure levels used in diagnostic ultrasound, there is no consistent evidence for adverse effects in tissues that are not known to contain stabilized gas bodies. Although modest tissue damage may occur in certain identifiable applications, the risk for induction of an adverse biological effect by a nonthermal mechanism due to exposure to diagnostic ultrasound is extremely small. *Key words*: cavitation; intestinal hemorrhage; lung hemorrhage; mechanical effects; nonthermal mechanism.

Abbreviations
ALARA, as low as reasonably achievable; CW, continuous wave; MI, mechanical index; PRF, pulse repetition frequency

Received April 12, 2007, from the National Center for Physical Acoustics, University of Mississippi, University, Mississippi USA (C.C.C.); Department of Electrical Engineering, University of Rochester, Rochester, New York USA (E.L.C.); Department of Physics, University of Vermont, Burlington, Vermont USA (W.L.N.); Department of Radiology, University of Michigan, Ann Arbor, Michigan USA (P.L.C.); Department of Electrical and Computer Engineering, University of Illinois, Urbana, Illinois USA (L.A.F.); and Center for Industrial and Medical Ultrasound, Applied Physics Laboratory, University of Washington, Seattle, Washington (M.R.B.). Revision requested April 18, 2007. Revised manuscript accepted for publication December 4, 2007.

Address correspondence to Charles C. Church, PhD, National Center for Physical Acoustics, University of Mississippi, 1 Coliseum Dr, University, MS 38677 USA.
E-mail: cchurch@olemiss.edu

CME *Article includes CME test*

Unlike most imaging modalities, diagnostic ultrasound necessarily induces mechanical strain in tissue. This strain is highest in proximity to gas or vapor bubbles. In the presence of ultrasound fields like those used in diagnosis, gas bubbles such as those in ultrasound contrast agents as well as naturally occurring gas bodies can damage adjacent tissue. In the case of micrometer-sized bubbles (ie, microbubbles) in general and contrast agents in particular, the damage is extremely localized, being confined to the immediate vicinity of the bubble, which is usually in a blood vessel. Sufficient information is now available concerning effects from contrast microbubbles, and they are potentially of such importance that they are the topic of a separate article in this issue (see Miller et al[34]). This review deals with potential effects resulting from the interaction of ultrasound fields with tissues containing naturally occurring gas bodies as well as tissues not known to contain gas bodies under normal physiologic conditions.

Fundamentals

As an ultrasound wave travels through a medium such as tissue, the pressure varies above and below the ambient value by an amount called the acoustic pressure. If the acoustic pressure is appreciably less than the ambient pressure, the wave propagates under linear conditions. Diagnostic techniques such as harmonic imaging make use of the nonlinear characteristics of propagation of large-amplitude signals. However, there is little evidence that nonlinear propagation plays a significant role in the nonthermal biological effects of ultrasound. Under linear conditions, in a continuous wave (CW) of a single frequency f, the acoustic pressure varies sinusoidally in time and space, the distance between consecutive maxima being the *wavelength* λ. When the wave is pulsed, the oscillations occur only during the pulses, the ratio of "on" time to "off" time being the *duty factor*. Current medical ultrasound uses longitudinal pressure waves. If a longitudinal pressure wave travels through a medium in the x direction, the "particles" (small-volume elements) that constitute the medium oscillate along that direction. Under linear conditions, the particle velocity in the wave varies sinusoidally in time and space with the same frequency and the same spacing as the pressure.

Newton's second law of motion describes the forward and backward motion of the particles that make up the propagating medium. When the mass involved is a part of a continuous sound-propagating medium, the appropriate form for Newton's second law is

$$F_V = \rho \frac{Du}{Dt}, \quad (1)$$

where F_V is the instantaneous force per unit volume; ρ is the density; and Du/Dt is the total derivative of the particle velocity u. At any instant, the density varies periodically along the direction of sound propagation, and at any position in the medium, the density varies periodically with time as the wave passes. The total derivative takes into account the fact that the particle velocity depends on both time and the field position of the particle of mass under consideration.

When the shear properties of the propagating medium can be neglected, the force F_V (per unit volume) that moves the particle in an acoustic wave traveling in the x direction is equal to the negative gradient of the scalar magnitude of the acoustic pressure ($-\partial p/\partial x$). This is a good approximation for the force per unit volume even with the viscous fluids and soft tissues that are the propagation paths for most diagnostic ultrasound.

As the wave (ie, the pattern of oscillating pressure and particle velocity) travels, potential and kinetic energy are imparted to the tissue or other medium through which it passes. It is shown in acoustic theory that the potential and kinetic energy densities for a plane wave are the same, and their sum, the total energy per unit volume E for a plane wave is equal to $\rho_o u_o^2$, where ρ_o is the equilibrium density, and u_o is the particle velocity amplitude. The wave and its energy move through the medium at the speed of sound c. The rate per unit area at which energy is transmitted across a boundary is called the *intensity* I and is equal to $E\,c$.

In the subsequent discussion, we shall use terminology from acoustic theory and refer to such oscillating quantities as the acoustic pressure and particle velocity as *first-order* quantities and

to the energy density E and intensity I as *second-order* quantities. A characteristic of a second-order quantity is that, like the kinetic energy density, it is proportional to the square of a first-order quantity, or, more generally, to a product of two first-order quantities. Quantities of both first and second order are relevant in discussing possible causes of biological effects. Adverse clinical impacts from these effects can be avoided without compromising diagnostic information. To do so, however, it is important that practitioners be aware of possible mechanical (as well as thermal) effects of ultrasound. Both first- and second-order phenomena are discussed in detail in National Council for Radiation Protection and Measurements report 140, *Exposure Criteria for Medical Diagnostic Ultrasound, II: Criteria Based on All Known Mechanisms*.[1]

Radiation Force

The force in Equation 1 that moves the particles forward and backward during wave propagation under typical diagnostic conditions (eg, 1 MPa at 2 MHz) is on the order of 10^{10} N/m^3 or about 1 million times the force that gravity would exert on the same material. Despite these huge forces, the particles shift only about 50 nm from their equilibrium positions as the sound passes through the medium. If the propagating medium is lossless, the time average of the acoustic forces is 0.

When some of the energy of the acoustic wave is absorbed by the medium and converted into heat, the time average of the force per unit volume on the medium has a small net value called the *radiation body force*, which is given by

$$F_{VR} = < F_V > = \frac{2\alpha I}{c}. \quad (2)$$

Here, α is the absorption coefficient of the medium, and c is the sound speed. Because F_{VR} is proportional to I, the radiation force is also a quantity of second order.

The intensity in the example above (1 MPa at 2 MHz) is approximately $3 \cdot 10^5$ W/m^2 (33 W/cm^2). With a typical absorption coefficient for soft tissue of 10 nepers/m, this gives a radiation force of about 4000 N/m^3, about half of the force that gravity would exert on the same material.

As the wave penetrates the tissue, its amplitude is reduced exponentially with depth (assuming a homogeneous path); hence, the radiation body force decreases in the same manner. The total force F_R exerted on the tissue from the absorption of all of the power W in the beam is

$$F_r = \frac{W}{c}. \quad (3)$$

Notice that Equations 2 and 3 are related by the volume within which the acoustic power is absorbed; multiplying a result obtained with Equation 2 by the volume of absorption yields the result given by Equation 3.

Human Perception

Radiation force has been perceived by human subjects in a number of instances at different thresholds. Some of these results are described here. For example, with a 1-cm^2 transducer coupled to the fleshy part of the forearm (avoiding bone in the path), subjects were able to perceive 10- to 100-millisecond pulses of 2-MHz ultrasound in which the power was greater than approximately 20 W, or a total radiation force of about 13 mN.[2] In those experiments, the radiation force was distributed over several centimeters of the sound path.

The fingertips are inherently more sensitive to tactile perception than the tissues of the forearm. In addition, anatomic and physical conditions increase the radiation forces at the fingertip over those in the fleshy part of the forearm. Bone has a much higher absorption coefficient than soft tissue, and, in addition, the acoustic impedance of the bone is about 3 times that of soft tissue, leading to reflection of a significant fraction of the incoming acoustic wave. The force required to reverse the direction of the wave is twice that needed to completely absorb it. Experiments were performed in which perfect reflectors of the ultrasonic wave were fixed to the fingertips of subjects. The material transmitted the radiation force exerted on it to the finger but reversed the direction of the wave. The highly localized force was

$$F_R = \frac{2W}{c}. \quad (4)$$

The results of these studies probably give us the lower limits of the force required for human tac-

tile perception of acoustic radiation force. Subjects were able to detect 2.2-MHz ultrasound administered in a single burst of 10 to 100 milliseconds above a threshold force of 3 mN or administered repetitively in 2.5-millisecond bursts at a repetition frequency of 200 Hz above a threshold radiation force of 0.5 mN (W = 0.4 W, equivalent to ≈0.7 W in the case of complete absorption).

The temporal characteristics of tactile perception are similar to neural responses to electrical stimuli. For steady-state fields, there is a broad maximum in tactile sensitivity at about 200 Hz, and for single pulses, thresholds are inversely related to pulse length Δt up to about 1 millisecond and relatively independent of pulse length for longer pulses.[2] Thus, the threshold for tactile perception is a constant radiation impulse ($F_R \Delta t$) ≈ 3 μN/s for Δt < 1 millisecond and a constant radiation force (F_R ≈ 3.0 mN) for Δt > 1 millisecond.

Lithotripter patients have no difficulty sensing individual pulses during their treatments; this sensation is likely the result of radiation forces generated in the body by the lithotripter pulse. However, in almost all diagnostic procedures, subjects are unable to perceive the acoustic radiation. Tactile perception presumably arises from membrane potential changes in specialized peripheral neural receptors. There is no basis for believing that radiation forces, even if perceived, are of more concern clinically than any other mild tactile stimulus.

Auditory receptors are the mammalian organism's most sensitive mechanical detectors. Higher frequencies and shorter pulses can be detected by the ear than by the finger. There are a number of reports of the detection of pulsed or sinusoidally modulated megahertz ultrasound by the human ear. As an example, Tsirulnikov et al[3] showed that the threshold ultrasound level varied with frequency of modulation in much the same way that the ear responds to audible airborne sound, with a broad minimum (maximum sensitivity) of about 1 W/cm^2 in the range from 200 to 4000 Hz. If the ultrasound in this experiment were completely absorbed in the outer ear, a radiation pressure (radiation force per unit area) on the order of 7 Pa would be generated there. Because this is very much greater than the threshold for hearing of airborne sound ($2 \cdot 10^{-5}$ Pa), it is reasonable to assume that the ear in these experiments was detecting the transmitted audio frequency radiation force generated by the ultrasound, and only a small fraction of the ultrasound energy was absorbed or back-reflected.

Although it is an interesting example of a biological effect of acoustic radiation force, the above experiment has little relevance to diagnostic ultrasound. Amplitude-modulated CW ultrasound and temporal-average intensities as high as 1 W/cm^2 are rare in diagnosis. There have, however, been reports of auditory sensation during clinical examinations.[4] Patients exposed through the *foramen magnum* at the base of the skull with 2-MHz pulsed ultrasound at temporal-average intensities up to 0.5 W/cm^2 heard tones that varied in frequency with the pulse repetition rate and in loudness with the intensity of the ultrasound exposure. These observations are consistent with a radiation force mechanism by which the momentum of an ultrasound field generates low-frequency impulses in the biological medium. The same mechanism has been credited with increased fetal movements during ultrasound examination.[5–7]

Bioeffects

Both tactile and auditory receptors have their maximum sensitivities in the audible frequency range. Thresholds for detection depend strongly on the temporal characteristics of the modulation of the ultrasound. Bone health requires the repetitive stresses that occur in exercise and daily activity. Numerous studies have shown that ultrasound applied with a pulse repetition frequency (PRF) of 100 to 1000 Hz and a duty factor of approximately 0.2 accelerates bone fracture healing.[8,9] For example, a 1.5-MHz 200-microsecond tone burst repeating at 1 kHz (pulse-average intensity = 150 mW/cm^2) accelerated the appearance of the fracture callus in humans,[10] and similar exposure conditions stimulated proteoglycan synthesis in vitro.[11] Ultrasound-stimulated synthesis of cell matrix proteoglycan, which is associated with accelerated fracture healing, appears to be mediated by intracellular calcium signaling.[12] The pulsed 1.5-MHz signal produces radiation force vibrations at 1 kHz, and it has been found that a square wave 1-kHz signal is similar to the pulsed 1.5-

MHz signal in inducing chondrogenesis in an in vitro model.[13] Parvizi et al[11] quantified the area of cartilage nodules formed by the chondrocytes, providing a measure of chondrogenesis, and showed that the pulsed 1.5-MHz waves (PRF = 1 kHz) increased the area of nodules more than 3-fold compared with control chondrocytes. Continuous wave ultrasound does not appear to be effective for bone healing, while shock wave devices designed similarly to lithotripters, also have been shown to accelerate bone growth and healing.[14,15] Because the average intensity for either pulsed ultrasound or shock wave devices is usually much less than is typical for physical therapy, and the temperature rise is unlikely to exceed 1.5°C, the mechanism appears to be nonthermal.[16] Radiation force appears likely to be the cause of the effect, although further evaluation is needed to establish force as the mechanism directly responsible for bone healing.

There is also evidence of the detection of very intense, unmodulated acoustic fields in the brain at frequencies much higher than the traditionally defined upper limits of hearing. Divers can hear sounds up to 130 kHz (E. Cudahy, PhD, written and oral communications, 2005). The perception of the sound as reported by divers is that of a very high pitch, but the apparent frequency changes little above 16 kHz.

Radiation forces induced by ultrasound pulses timed to coincide with the moment of contraction of the frog heart have been shown to reduce the strength of contraction.[17,18] The effect required a minimum pulse duration of 5 milliseconds, which is orders of magnitude longer than typical diagnostic pulses. Therefore, there is no reason to assume that the effect will occur in the human heart under diagnostic conditions.

Radiation forces from short pulses of high-frequency, high-intensity focused ultrasound have been shown to move detached retinas and cause blanching (reduction of blood flow) of the region.[19,20] The conditions of exposure approach those that produce irreversible lesions in the eye.[21]

Radiation forces within standing wave fields, where there is no large-scale transport of momentum, are somewhat more complex than those described above for traveling waves.[22,23] Particles much smaller than the acoustic wavelength that are denser than the suspending fluid are forced to pressure minima in such a field. Using a specially designed exposure chamber, Dyson et al[24] showed that this mechanism caused banding and stasis of blood cells in chick embryos. This phenomenon is unlikely to have significance in typical diagnostic examinations for at least 3 reasons related to the physical aspects of exposure. First, for standing waves to form, there must be a reasonably well-defined specular reflector. Bone and possibly some locations on the surface of the lung satisfy that requirement to some degree. Second, the standing wave, such as it is, would be confined to the region of overlap of the incoming and reflected pulses, effectively somewhat less than half of the length of the pulse. For the longest pulses used in diagnosis, this would be less than 5 mm. Third, with typical scanning procedures, the beam would not remain stationary long enough for stasis to occur.

Sustained radiation forces on liquids may result in macroscopic streaming.[25] Investigators have taken advantage of this phenomenon to differentiate between fluid-filled cysts and solid lesions.[26–28] Investigators have also used radiation force directly in imaging. In this technique, known as acoustic radiation force impulse imaging, tissue is "pushed" from its equilibrium position with a long acoustic pulse. After the pulse, the tissue slowly moves, or "relaxes" back to its original position. The relaxation movement is detected by shorter probing pulses, and information on the elastic properties of the tissue is obtained.[29,30]

Implications

Acoustic radiation forces, which arise when acoustic waves are absorbed or reflected, can under certain circumstances be detected. In each case, there is a threshold that depends on acoustic pressure, PRF, and pulse duration. However, in normal diagnostic procedures, the magnitudes of the radiation forces are small, and their effects, if any, do not impact negatively on the medical use of ultrasound. One possible exception to this general conclusion concerns the interaction of diagnostic ultrasound with the large gas bodies present in the lung and intestine. This is discussed in detail below.

First-Order Acoustic Phenomena

In contrast with second-order radiation forces, the first-order forces that are used routinely in diagnostic procedures are very large. The 2- to 3-MPa pressures that are common in imaging and Doppler ultrasound are greater by 10^{11} than the threshold for hearing of airborne sound and greater than the threshold for pain for airborne sound by 10^5. The acoustic pressures used in lithotripsy are greater than diagnostic levels by an order of magnitude or more.[31] Instantaneous first-order body forces, the forces that cause the elements of the tissue to oscillate back and forth along the direction of propagation, are directly proportional to the acoustic pressure and the frequency of the ultrasound. For 1 MPa at 1 MHz, these forces are greater than the forces of gravity on the same material by $4 \cdot 10^5$.

However, most tissues in the body are exposed routinely to diagnostic ultrasound with no apparent adverse biological effects. It is not the forces per se, of course, but their physical effect on the tissue that leads to biological effects. Ultrasound propagating in a medium, such as tissue, causes the constituent molecules to move closer together and farther apart. These displacements are oscillatory and tiny (≈0.1 μm for a 1-MHz pulse at 1 MPa); they produce no lasting effect. For high-intensity ultrasound or lithotripter pulses, the displacements are greater, 1 to 100 μm, and the accelerations producing them are very large. These displacements and accelerations, in combination with internal heterogeneity in the cellular structure, have been used to explain the disruption of cells observed after exposure to high-amplitude pulses.[32,33] Inhomogeneities, in particular gaseous inclusions, can amplify and distort the particle motion. Almost every adverse biological effect of diagnostically relevant ultrasound that has been identified has been associated with some form of included gas. Before proceeding further with an exploration of mechanically produced biological effects, it will be useful to provide some information about how bubbles respond to acoustic fields.

Response of Bubbles to Acoustic Fields

Theory

There is a large body of theoretical analysis and experimental data on the interactions of individual gas-filled microbubbles with acoustic fields. These may be present naturally in the body (eg, in the lung or intestine); they may be produced by the passage of an acoustic wave of sufficient intensity (eg, in the kidney during shock wave lithotripsy, either from preexisting cavitation nuclei or spontaneous nucleation in regions of low interfacial tension); or they may be produced by an external process and subsequently may be introduced into the body (eg, by intravenous injection of ultrasound contrast agents).[34] In this work, the term *gas body* is sometimes used to represent any physically contiguous collection of gas molecules without restriction on size or shape and which may be acted on by the acoustic field. Thus, both the lung as a whole and the individual microbubbles constituting an ultrasound contrast agent, as well as anything in between, are considered gas bodies. To differentiate between the general term *gas body* and the specific term *gas bubble*, we simply require that the latter be completely surrounded by either fluid or tissue or both and that it be small in comparison to the acoustic wavelength.

A bubble in a sound field is acted on by acoustic stress at its surface. Because a bubble is composed of highly compressible gas, this time-varying acoustic pressure produces relatively large oscillations in the bubble volume. At low pressures, the motion of a bubble having equilibrium radius R_0 and suspended in a liquid of density ρ_0 is well described by the equation for a damped linear harmonic oscillator:

$$m\ddot{x} + b\dot{x} + k_s x = -4\pi R_0^2 p_A \cos \omega t \,, \quad (5)$$

where $x = R(t) - R_0$; m is the effective mass ($= 4\pi R_0^3 \rho_0$); b is proportional to the damping; k_s is the stiffness (equivalent to a spring constant in a spring bob oscillator); p_A is the acoustic pressure amplitude; and ω is the angular frequency ($= 2\pi f$). Equation 5 is an expression of Newton's first law: $F = ma$. The three terms on the left side of Equation 5 represent the effective mass times the net acceleration, the damping force (caused

by several mechanisms), and the outward force exerted by the gas within the bubble, respectively, while the term on the right side gives the force exerted on the bubble by the surrounding liquid. A solution to Equation 5 is

$$x = x_0 \cos(\omega t + \beta), \tag{6}$$

where x_0 is the amplitude of the radial displacement, and β is the phase angle between the driving pressure wave and the displacement. These have the following forms:

$$x_0 = \frac{p_A}{\rho_0 R_0 \sqrt{\left(\omega_0^2 - \omega^2\right)^2 + \omega^2 b^2 / m^2}} \tag{7}$$

and

$$\beta = \arctan\left[\frac{\omega b}{m\left(\omega^2 - \omega_0^2\right)}\right], \tag{8}$$

where $\omega_0^2 = k_s/m$, and $f_0 = \omega_0/2\pi$ is the resonance frequency. Bubbles exhibiting the largest radial response for low driving pressures at a particular acoustic frequency (eg, in blood), bubbles of approximately 3.9 μm in diameter at 2 MHz, are said to be of resonance size. The spherical bubble motion is damped (ie, loses energy) because of 3 primary mechanisms: viscous damping arising from the viscosity of the liquid that is forced into motion by the pulsating bubble, radiation damping from the acoustic wave emitted by the pulsating bubble itself, and thermal damping arising from a net transfer of heat out of the bubble and into the liquid. More thorough treatments of this problem are widely available.[1,35–37]

For small pressures where Equation 5 is applicable, a bubble is said to oscillate "linearly," and a plot of the radius versus time will be a simple sinusoid centered about the bubble's equilibrium radius R_0. On the other hand, exposure to a sufficiently high acoustic pressure will induce higher-amplitude, nonlinear oscillations in the bubble volume. These two situations are illustrated in Figure 1 for a 4-μm-diameter spherical bubble exposed to 2-MHz acoustic waves having pressure amplitudes of either 0.01 or 0.5 MPa. While the response to the lower pressure is sinusoidal as expected, the response to the higher pressure is characterized by high-amplitude, long-duration (ie, greater than half of an acoustic period) excursions above the equilibrium radius separated by relatively brief intervals below it. As the bubble contracts from a radial maximum to the subsequent minimum, the motion of the surrounding fluid may attain such a large momentum that the rising pressure within the bubble, which easily counteracts this momentum at low acoustic intensities and thus produces a balanced (sinusoidal) oscillation, cannot withstand the inrushing liquid. The bubble's radius very rapidly becomes extremely small; that is, the bubble "collapses." This is termed an *inertial collapse* because the motion is dominated by the inertia of the liquid. This concept is used to differentiate two classes of cavitation fields: *noninertial cavitation* when bubble motion does not involve inertial collapse and *inertial cavitation* when inertial collapse does occur. As might be expected, the mathematical description of bubble activity at higher pressure amplitudes is much more complicated, but again several authors have treated the problem,[38–41] while Prosperetti and Lezzi[42] have shown that these formulations are essentially equivalent.

Cavitation Thresholds

Theoretical results from this research indicate that there is often a rapid increase in radial response with only a very modest increase in the amplitude of the acoustic field; the effect is par-

Figure 1. Predicted radial responses for a bubble having a diameter of 4 μm and exposed to a 5-microsecond pulse of 2-MHz ultrasound having an acoustic pressure of 0.01 MPa (thick line) or 0.5 MPa (thin line). The former illustrates a harmonic linear response, while the latter exhibits strong nonlinearity and several inertial collapses.

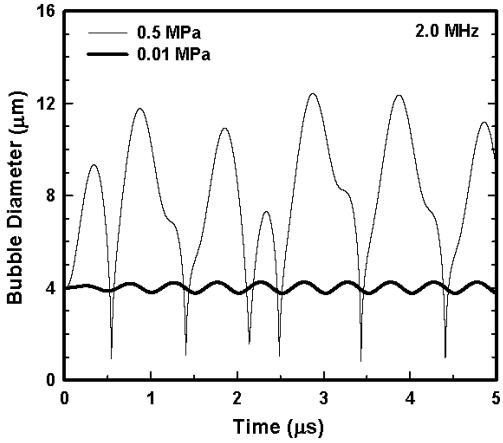

ticularly strong for small bubbles (ie, those below the linear resonance size).[43] The acoustic pressure at which this rapid increase in response occurs is loosely termed the *cavitation threshold* or, more precisely, the *threshold for inertial cavitation*.[44] Theoretical results indicate that inertial cavitation should be produced quite readily by diagnostic exposures of pure liquids given the presence of appropriate cavitation nuclei.[45–48] The cavitation threshold is approximately 0.2 MPa at 1 MHz for a 1-cycle pulse, decreasing to as little as 0.12 MPa as the pulse length increases.[49] However, it is clear that pure liquids are rare in the human body. Body tissues are viscoelastic solids, and recent modeling indicates that the cavitation thresholds for soft tissues will be higher, and sometimes much higher, than those for liquids even when optimally sized nuclei are present[50]; the difference in response is primarily due to the rigidity of the tissue that constrains the bubble motion. The theoretical result is consistent with animal studies of shock wave lithotripsy in which cavitation is observed first in the collecting system of the kidney,[51] and tissue injury is seen in vessels and tubules within the tissue.[52] In addition, there is little evidence for the presence in vivo of cavitation nuclei that may be excited by diagnostic ultrasound, although cavitation can be detected immediately in the urine in pig kidneys during shock wave lithotripsy.[51,53,54] In the absence of preexisting nuclei, the minimum cavitation threshold for microsecond-long pulses of 1-MHz ultrasound is at least 4.0 MPa, a value obtained by combining observations of cavitation during clinical lithotripsy procedures with theoretical analyses of spontaneous nucleation and bubble dynamics in liquids.[55] The fact that the experimental threshold for tissue damage in a variety of laboratory animal models exposed to millisecond-long pulses of megahertz-frequency ultrasound is more than an order of magnitude greater than the threshold in water is taken as evidence that preexisting, gas-filled nuclei are not usually present in vivo (see "In Vivo Effects, Soft Tissue: Gas Free" below for a review of this literature).

Potential Mechanisms for Biological Effects

The mechanisms by which a bubble may affect nearby biological material are dependent on the magnitude of the bubble's response to the acoustic field. Essentially all bubbles produce acoustic radiation forces and microstreaming, while only the more strongly affected will exhibit the violent responses (eg, shock wave generation or free radical production) characteristic of inertial cavitation. Descriptions of these effects follow.

Radiation Forces

In the same way that absorption of an acoustic wave by tissue causes a decrease in the forward momentum of the wave, which is recognized as an "effective force" on the tissue called the radiation force (see Equation 1), so too does a bubble absorb an acoustic wave and thereby decrease its forward momentum. This effect is also perceived as an effective force, a radiation force on the bubble. The method for calculating this force is similar to the method for tissue. Equivalent to the absorption coefficient for tissue is the extinction cross section σ_e, which quantifies the ability of a bubble to remove energy from a wave (ie, to decrease the wave's momentum). Multiplying σ_e by the incident intensity I gives the rate at which energy is removed from the wave, equivalent to the numerator in Equation 1, $2\alpha I$, which is the rate at which a unit volume of tissue removes energy from the wave. Dividing by the speed of sound c gives the radiation force $\sigma_e I/c$ for a bubble and $2\alpha I/c$ for a unit volume of tissue. For low-amplitude acoustic fields, a simple analytical expression for σ_e may be obtained from Equation 4. This expression shows that near resonance, the extinction cross section of a bubble is many times greater than its physical cross section and thus that the force is much greater than might be imagined. For higher-amplitude pulsations, the extinction cross section and thus the force must be computed numerically.

It is found that radiation force can cause a bubble to move at high speed (≈10 m/s) in a cell suspension exposed to ultrasound under typical in vitro experimental conditions. Cells near the path of a speeding bubble may be damaged by exposure to high shear stresses as it passes.[56]

There are many predictable phenomena for bubbles and the materials around bubbles. A pulsating bubble itself acts as a source of acoustic waves, reradiating, or scattering, a part of the acoustic energy that it absorbs. If a second bubble happens to be near the first, this scattered

wave will exert a force on the second bubble; the "second" bubble also exerts a force on the first. If the two bubbles are both smaller or larger than the resonance size, the net force will be attractive, and the bubbles will move toward one another. This force is responsible for one of the possible mechanisms whereby bubbles in a sound field may grow because if the two bubbles touch, they may coalesce into a single larger bubble. If one of the bubbles is larger than the resonance size and the other is smaller, the smaller will be attracted to the larger when the two are closer together than about 0.8 times the radius of the larger bubble, but it will be repelled for larger separations.[57]

The acoustic wave scattered by a bubble may also affect small particles (eg, biological cells) that happen to be near the bubble. For particles denser than the suspending medium, which includes most cases of biological interest, the direction of the force is toward the bubble, while the magnitude of the force decreases as the fifth power of the distance from the center of the bubble.[57] Oscillating bubbles will tend to attract nearby particles or cells, thus collecting them into small, highly concentrated groups where they may be more easily damaged or destroyed by the pulsating bubble. However, the oscillation of a bubble may be reduced by material accumulating on its surface, thereby reducing the extent of any damage that may occur.[58–60]

Microstreaming

Bubbles oscillating in a sound field, especially if they are located on a solid surface, produce a vigorous small-scale circulatory motion in the surrounding fluid.[61–64] Such fluid motion is called *microstreaming*. Oscillating bubbles that are being pushed by a traveling wave also may produce shearing flow in the surrounding fluid, although this motion is noncirculatory. In all cases, because the velocity of the fluid flowing around the bubble is greatest near the bubble surface, and because the fluid velocity decreases as the distance from the bubble increases, a gradient exists in the fluid flow field around the bubble. When a cell is carried by the streaming flow into a region of strong fluid velocity gradients, the fluid will exert greater force on the side of the cell near the bubble and less force on the side farther away. This unequal distribution of forces on the exterior of the cell results in shearing stresses (or forces) that tend to distort and tear the cellular membrane. Because cells have viscoelasticity, some minimum time is required for a given level of shear stress to disrupt a membrane; typical minimum times for hemolysis are 1300 microseconds at 0.45 kPa and 25 microseconds at 0.1 MPa.[62]

Shock Waves

During an inertial collapse, the speed of the gas-liquid interface may be very high, in some cases becoming supersonic in both the gas (>330 m/s) and the liquid (>1500 m/s). Such supersonic motion can produce shock waves both within the bubble and in the surrounding fluid. The external shock will propagate outwardly as a spherically diverging wave. A biological cell or tissue exposed to the shock will briefly experience very large stresses and spatially varying body forces. For a shock wave generated by a lithotripter, the shock thickness measured in vivo was 150 nm,[65] and shock waves generated near a bubble collapse may be even thinner. Hence, a pressure difference on the order of 10 MPa can exist inside a cell, thereby subjecting the cellular contents at the shock front to a body force of greater than $7 \cdot 10^{13}$ N/m^3. Because the individual components of the cell have different densities, they may be displaced to different degrees by this body force. Forces of this magnitude can break the cell whether the shock is generated by a bubble collapse or the acoustic source itself. Lokhandwalla and Sturtevant[66] proposed a mechanism for tissue damage by a lithotripter shock wave in which the very narrow shock front was superfocused by inhomogeneities in tissue (termed *wave front folding* in the case of sonic booms propagating in a turbulent atmosphere). The focusing creates pressure gradients and shear within cells, tissues, and blood vessels. The authors then expanded this idea to show that the shock wave source might be a cavitation bubble[67] and therefore that the effect might also occur during diagnostic examinations. Overpressure experiments in cell suspensions confirm a minimal level of lysis attributed to shear when thermal and cavitation effects are suppressed.[68] As with microstream-

ing, creation of a significant pressure gradient across the cell causes distension of the cell, and at some threshold level, the gradient is strong enough, and the distension great enough, to tear the cell. In addition, inhomogeneities in the tissue (eg, structural fibers or blood vessels) may further concentrate these stresses and thus amplify the effect.

Free Radicals

When a bubble undergoes inertial collapse, there is a brief time (on the order of nanoseconds in duration) near the radial minimum during which the pressure within the bubble may rise to hundreds or thousands of megapascals, and the temperature may reach thousands of kelvins. In addition to various gases, such as nitrogen, oxygen, and argon, and various fluorocarbons in the case of ultrasound contrast agents,[34] the interior of a bubble contains water vapor. The existence of high temperatures in such an aqueous medium may lead to the formation of chemically reactive free radicals, such as •H and •OH, by the dissociation of water.[69–71] Although these free radicals would be very damaging to any biological tissue they should encounter, they tend to have extremely short lifetimes in vivo ($\approx 10^{-9}$ second, equivalent to a mean free path of ≈0.5 μm). However, hydrogen peroxide, which may be produced by recombination of the appropriate free radicals, is another product of cavitation. This molecule is long lived and has been shown to induce single-strand breaks in DNA in vitro.[56] One may speculate that any of these chemical species produced by the action of the sound wave (ie, any of these "sonochemicals," as well as many of the others produced by inertial cavitation) may injure biological cells or tissues in the vicinity of a collapsing bubble, particularly if the bubble collapses inside the cell. This damage may result from the direct effect of a sonochemical on a biological molecule such as DNA, thus resulting in a potential genetic effect, or the action may be indirect, involving the production of potentially toxic secondary chemicals (eg, radical adducts).[72] However, intensive investigations in vitro have shown that it is very difficult to induce genetic mutations in intact cells even for exposure levels far above those permitted in diagnostic ultrasound examinations.[73,74]

Microjets

Most theoretical analyses of bubble-mediated ultrasound bioeffects assume that the bubble remains spherically symmetrical throughout its motion. While this assumption is valuable in that it allows detailed investigations of various aspects of cavitational activity, bubbles in the relatively strong acoustic fields common to biomedical ultrasound probably do not remain completely spherical. The threshold for the generation of surface waves on the bubbles is much below the intensity of typical biomedical exposures,[57] and the amplitude of the waves increases with the acoustic driving pressure. At high amplitudes, surface waves become distorted. Bubbles may be pierced by liquid jets, ruptured into many daughter bubbles, or both. The generation of daughter bubbles is important because they may act as nuclei, or "seeds," from which additional biologically damaging cavitation bubbles may develop. Small liquid jets, called *microjets*, may also produce significant biological effects.

When a bubble located on or near a solid boundary is exposed to an acoustic wave, it expands and contracts in response to the time-varying pressure, as would any other bubble. In this case, however, while the fluid opposite the boundary is free to flow toward the bubble's center, the solid surface restricts the motion of fluid on that side of the bubble. This asymmetry distorts the bubble interface in such a way that an invagination of fluid forms on the side of the bubble opposite the boundary. As the acoustic pressure is increased, this distortion is magnified until the liquid flows completely through the bubble and impacts the solid boundary. Such events are known to be very violent, being able to pit brass plates and pierce aluminum foils.[75] Although the relevance of microjet activity to ultrasound bioeffects research remains to be determined, Kodama and Takayama[76] have shown that microjets will be directed toward nearby compliant surfaces such as vascular epithelia, and considerable tissue damage may result.

Strain

Separate from studies showing tissue damage from the fluid jet impact of a collapsing bubble, there are several in vitro experiments that have

measured strain and rupture of tissue or tissue phantoms induced by bubble oscillation. The oscillations of a bubble within a fluid that is in contact with a tissue surface strain that tissue. Using a polariscopic technique, Delacretaz et al[77] measured relative strain induced in a polyacrylamide tissue phantom by an oscillating bubble. The highest tensions, displacements, and macroscopic damage to the gel were observed as the bubble collapsed, drawing fluid inward and pulling on the tissue. Compression was seen as the bubble expanded. Lokhandwalla and Sturtevant[67] and Gracewski et al[78] calculated the elongational and shear strain induced in a red blood cell by the asymmetric fluid flow field induced by oscillation and shock wave emission of a cavitation bubble. Experiments showed that such spatial pressure gradients produced hemolysis,[68] supporting earlier results from Rooney,[61–63] who had used flow generated by an oscillating bubble to measure shear injury to blood cells. In fact, it appears that little fluid between the bubble and the tissue is necessary to strain or rupture the tissue. Zhong et al[79] filmed the expansion of acoustically excited microbubbles and the subsequent distension of a plastic tube surrounding them. Their design of a lithotripter pulse intended to minimize bubble expansion resulted in fewer ruptured vessels in animal studies. Carstensen et al[80,81] had earlier proposed that a similar mechanism, the ultrasonically induced expansion of a preexisting gas body, could produce the tissue injury observed in *Drosophila* larvae. While it may be difficult to conceive that a nearly empty bubble can push on tissue strongly enough to damage it, the concentration of applied stress near a void and the resulting strain in the surrounding material are generally accepted to be how fractures grow in brittle materials[82,83]; a similar mechanism has been proposed for tissue.[66] Therefore, the asymmetry of fluid flow or hydrodynamic pressure created by oscillating bubbles will certainly stress, and may then shear, biological tissue.

In Vivo Effects

There is considerable evidence relating the presence of microbubbles to a variety of biological effects of ultrasound, in many cases under diagnostically relevant exposure conditions. However, much of this work was performed in vitro, and its relevance to diagnostic exposures of adult humans is not clear because large numbers of gaseous microbubbles are not known to be present under normal conditions. An important exception occurs with the use of ultrasound contrast agents, a subject discussed in some detail by Miller et al.[34] The relationship between exposures to diagnostic ultrasound and acoustic cavitation is treated below insofar as it relates to the healthy adult.

Blood

It appears that in normal mammalian tissue and blood, micrometer-sized bubbles are extremely rare. Cavitation is seen readily and immediately in the urine of the kidney collecting system during shock wave lithotripsy, but it is only detected much later in tissue, after hundreds of shock waves. If this were not true, certain high-intensity diagnostic procedures probably would have produced noticeable tissue damage. Blood, in particular, seems to be largely free of small bubbles. It is, of course, the body's transport medium for gases, but it appears that most if not all of those gases are dissolved or chemically bound. Using a resonant-bubble detector located on the abdominal aortas of dogs, Gross et al[84] were unable to detect cavitation bubbles in heart or aortic blood exposed to 0.5- to 1.6-MHz, CW ultrasound up to 16 W/cm^2 (0.7 MPa). Using a similar detector, Gross et al[84] were also unsuccessful in attempts to identify cavitation from left ventricular blood in dogs exposed to 0.75- and 1.45-MHz ultrasound up to 1 kW/cm^2 (5.5 MPa). Ivey et al[85] recorded images of bubble boluses produced by a 15-millisecond pulse of 1.8-MHz ultrasound at 19 kW/cm^2 (23 MPa). Recently, Hwang et al,[86] using a passive cavitation detector operating at 5 MHz, detected an increase in the inertial cavitation rate in the auricular veins of rabbits exposed to 500-cycle, 1-kHz-PRF pulses of 1.17-MHz ultrasound at a rarefactional acoustic pressure p_r of 6.5 MPa but no increase at a p_r of 3.0 MPa; the threshold was a p_r of less than 1.0 MPa in the presence of the microbubble contrast agent Optison (GE Healthcare, Princeton, NJ).

Soft Tissue: Gas Free

High-intensity focused ultrasound can be used to necrotize tissue and form thermally coagulated lesions by conversion to heat of absorbed ultrasound energy. Short bursts of focused ultrasound produce negligible heating but can create lesions due to bubble nucleation and subsequent cavitation. Lesions induced in soft tissues by heating are characterized by smooth boundaries, while those produced by cavitation usually are irregular. Fry et al[87] and Dunn and Fry[88] induced cavitation in cat brains with 1-MHz CW exposures of a few milliseconds' duration at 2 kW/cm^2 (8 MPa). A sharp, audible "snap" correlated with the appearance of irregular lesions, consistent with a cavitational mechanism, and the lesions did not necessarily appear at the focus but rather at the interfaces between neural tissue and fluid-filled spaces such as ventricles and blood vessels. Frizzell[89] reported similar results for CW exposure of cat livers at 3 MHz, with a threshold intensity for cavitation involvement that was less than 2 kW/cm^2 (7.7 MPa calculated assuming linear propagation, which overestimates the rarefactional pressure) for 30-millilsecond pulses. Taylor and Pond[90] found disruption of the normal cellular architecture around the central vein of rat livers after 5-minute exposures to 10-millisecond pulses of 1.3-MPa ultrasound at 0.5, 1.0, and 2.0 MHz. The number of lesions decreased with increasing frequency, and none were observed at 6.0 MHz; this frequency response is indicative of cavitational activity. Lee and Frizzell[91] reported the threshold level for cavitational involvement in hind limb paralysis of the mouse neonate due to CW exposure of the spinal cord to be approximately 1.5 MPa at 1 MHz for exposure durations of about 1 second at 37°C. However, Frizzell et al[92] later used the same animal model to examine thresholds with pulsed ultrasound. Using 1-MHz pulsed ultrasound with a 10-microsecond pulse duration and a 2.4-second exposure duration at 10°C, they found that the threshold peak rarefactional pressure for cavitational involvement in the paralysis was greater than 5.1 MPa for a 5-kHz PRF. The threshold decreased as the PRF was increased, suggesting that the threshold would be even higher if the PRF were reduced to 1 kHz, more typical of diagnostic ultrasound. In general, the studies using pulsed exposures are more indicative of what would be expected from diagnostic ultrasound because heating associated with CW exposures can increase the likelihood of cavitation by increasing the prevalence of nuclei.

In experimental hyperthermia procedures in dog muscle, Hynynen[93] noted the sudden onset of subharmonic emissions (a common indicator of cavitation) from the focal region and a simultaneous marked increase in scattering, attenuation, and the rate of heating for 1-second exposures. Thresholds were approximately 300 W/cm^2 (3 MPa) at 0.5 MHz and 800 W/cm^2 (5 MPa) at 1 MHz. In addition, a kind of hysteresis was observed, with higher thresholds being observed when the acoustic pressure was increasing and lower thresholds when it was decreasing from levels above the initial threshold. Tissue emulsification has been observed with pulsing schemes involving a repeated sequence of one high-amplitude "primary" pulse followed at the mid period by one lower-amplitude "cavitation-sustaining" pulse.[94] Porcine myocardium exposed to 5×10^4 17-microsecond-long pulses of 750-kHz ultrasound at a PRF of 0.33 kHz with primary and cavitation-sustaining amplitudes of 17 and 4.5 MPa, respectively, was eroded completely away by inertial cavitation but formed solid, apparently thermal lesions for cavitation-sustaining pulse amplitudes above 9.0 MPa.[95] Cavitation has also been detected in the kidney parenchyma of pigs during lithotripsy but only after many shock waves.[51] Perhaps not coincidently, vascular injury to pigs in the Dornier HM3 lithotripter (Dornier MedTech, Kennesaw, GA) has only been sufficient to quantify after many shock waves.[52]

While it requires rather substantial acoustic pressures to damage biological tissues, simple bubble growth apparently may be induced in vivo at much lower levels. ter Haar and Daniels[96] and ter Haar et al[97] reported that exposing the hind legs of guinea pigs to 0.75-MHz CW ultrasound caused the appearance of new echoes on an 8-MHz pulse echo imager capable of detecting bubbles of 10 μm or more in diameter. The threshold was 80 mW/cm^2 (0.05 MPa), and the number of bubbles detected increased with intensity up to 680 mW/cm^2 (0.14 MPa). The detection of new echoes (ie, microbubbles) was

suppressed by the application of hydrostatic pressure, a classic test for cavitational activity. The same authors also reported that the threshold for pulsed ultrasound (2-millisecond pulses and 50% duty cycle) was approximately 240 mW/cm^2 (0.08 MPa). Although these studies did not involve tests for biological effects, they are important because they provide evidence for the existence of cavitation nuclei in tissues.

Soft Tissue: Gas Containing

In contrast to the tissues discussed above, some body structures contain copious amounts of undissolved gas. For example, the lung is largely gas. Rather than being the micrometer-sized spherical bubbles in an infinite fluid medium as idealized in the theory above, most of the gas in the lung is contained in comparatively large alveoli, surrounded by other gas-filled alveoli and therefore not in an environment favorable to inertial cavitation. Bacterial action within the contents of the intestine produces bubbles with a nearly continuous distribution of sizes. Some of these bubbles are near the walls of the lumen and in an environment that can support inertial cavitation. That nuclei exist in other parts of the body is attested by the physics of decompression illness.[98,99] However, the concentration and distribution of gaseous micronuclei in the body remain somewhat a mystery. Because these tissues may be more easily affected by diagnostic exposures than apparently gas-free tissues, they will be treated more extensively.

Lung Hemorrhage

In the normal healthy subject (absent exogenous contrast agents), there is little basis for concern about mechanically induced biological effects of ultrasound in most diagnostic procedures. The organ most vulnerable, however, is the lung. This was shown in the initial studies of biological effects on the lung of the mouse.[100] As a result of the low threshold for hemorrhage in the lung and a desire to determine the responsible mechanism, the lung has become one of the most examined organs for biological effects studies. Studies have been conducted by several different laboratories using a variety of experimental animals ranging in size from newborn mice to 60-kg pigs. Studies included monkeys,[101] mice,[18,100,102–106] rats,[106–116] rabbits,[105,117] and pigs.[118–120]

An example of lung hemorrhage is shown in Figure 2, and the penetration into the lung is shown in Figure 3.

Although thresholds for lung hemorrhage appear to be lower than exposure levels extant in diagnostic equipment used on humans, lesions are small, do not appear to affect function,[108] and are repaired by the body within a few weeks.[109] In the large database of lung hemorrhage studies, there is no clear dependence of threshold on the species of the laboratory animal. Within the range of interest for most diagnostic examinations, neither is there a clear dependence on frequency of exposure. Although the superthreshold damage increases with pulse duration and total exposure time, the threshold itself is only weakly dependent on these parameters.

The body of literature providing thresholds for hemorrhage in lung from exposure to acoustic waves is huge, ranging from audible[121] and low[122] ultrasonic frequencies to several megahertz. To simplify analyses of these data for purposes of this document, the frequency range will be restricted to 1 MHz and above. The available data for the threshold for lung hemorrhage at diagnostically relevant frequencies are tabulated in Table 1. Even in this frequency range, the variation in exposure parameters is very large. The data as a whole contain a range of pulse durations, exposure durations, beamwidths, and PRFs. The threshold results show the following general trends. Thresholds decrease slightly but consistently with pulse length and are indepen-

Figure 2. Lateral view of rat lung exposed to pulsed ultrasound under superthreshold conditions. Note the circular area of subpleural hemorrhage that radiates centripetally from the center of the exposure beam (darker red area) to the periphery (lighter red area). Scale bar indicates 5.5 mm.

dent of beamwidth (although the superthreshold lesion size is dependent on beamwidth). For all studies, however, once the acoustic pressure exceeds the threshold for lung hemorrhage, the extent of damage depends strongly on pressure.

Some additional insight on thresholds may be gained by selecting a subset of the data in the diagnostic frequency range representing two extremes of exposures that exist in the literature. The first group (labeled A in Figure 4) includes exposures with pulse durations on the order of 1 microsecond at a 1000-Hz PRF and exposure durations on the order of 10 seconds. The second group (labeled B in Figure 4) includes exposures with pulse durations on the order of 10 microseconds at a 100-Hz PRF and exposure durations of 3 minutes. Thresholds for these two sets of experiments are summarized in Figure 4. Although the total on time (product of pulse duration, PRF, and exposure duration) for sound in group B is roughly 15 times greater than for group A, the thresholds for the two groups differ by only a factor of approximately 3. For example, at 3 MHz, the threshold for long exposures may be rounded to approximately 1 MPa, while the threshold for short exposures centers around 3 MPa. It is concluded that the threshold for damage decreases as the exposure duration or the pulse length increases.

Figure 3. Histologic section through hemorrhage induced in rat lung exposed to pulsed ultrasound under superthreshold exposure conditions. Scale bar indicates 200 μm. Inset, Enlargement of the pleural surface in the region of damage. Scale bar indicates 20 μm. Note the accumulation of red blood cells in the alveoli. Hematoxylin-eosin stain.

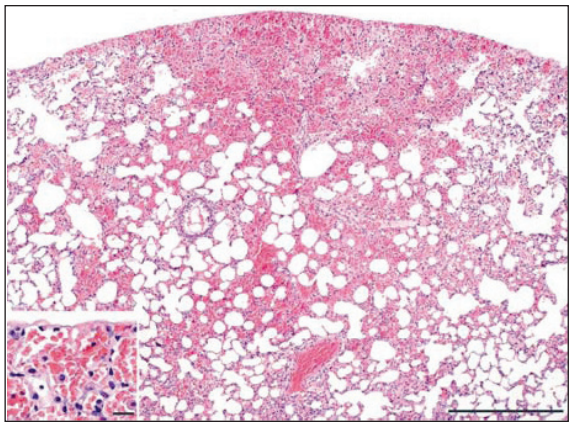

In contrast with thermal damage, hemorrhage can occur with very short exposures and very little acoustic energy delivered to the tissue. The degree of superthreshold damage depends on acoustic pressure, total exposure time, and beamwidth. The question of mechanisms is discussed in greater detail below.

Of course, comparable investigations with human subjects have not been conducted. One study involving patients that had been exposed to observations of the heart with ultrasound in preparation for open heart surgery had negative findings; of 50 subjects, none showed any evidence of lesions on the surface of the lung.[123] The upper limits of lung exposure in that study were estimated to be approximately equal to the threshold for hemorrhage in laboratory animals. From this, we may conclude that human lungs are not anomalously much more sensitive than those of laboratory animals.

Relating Output to Threshold

If this information is to be useful, we first must assess the probability that there will be a biological effect, in this case, whether the acoustic pressure at the surface of the lung exceeds the threshold for lung hemorrhage. Then, the magnitude of any adverse effect must be assessed. Combining the probability of harm and the magnitude of that harm provides a measure of the risk to the patient from the diagnostic exposure. If the probability is nonzero, the risks or possible risks to the patient must be balanced against the benefits of the examination. Evaluation of risk versus benefit is largely a qualitative process involving informed judgment of the operator. We can, however, relate quantitatively the experimentally determined thresholds for lung hemorrhage shown in Figure 4 to values of output shown on-screen in specific exposure situations. These relationships depend on assumptions for geometry of the tissue path and sound beam and the attenuation characteristics of the tissues through which the sound passes. This must be done in any application; however, the relationship between output and exposure is particularly contorted in the case of the lung.

Lung exposure in routine practice is confined almost exclusively to echocardiography. Within this discipline, transdermal and transesophageal examinations of the heart present different

anatomic pictures. In either case, the lung may be exposed either in the near field of the transducer or at the distal surface of the heart after the sound beam has passed through heart muscle and blood.

Information on machine output relevant to lung exposure comes to the operator as the mechanical index (MI). The MI was formulated with a simple homogeneous organ such as the liver in mind. In that application, the MI multiplied by the square root of the frequency would give a reasonable approximation to the negative acoustic pressure at the focus of the transducer. Almost nothing that entered into the definition of MI is relevant to exposure of the lung in echocardiographic applications. Therefore, one must "undo" the on-screen MI information to get the original output information and add several assumptions about the geometry of the field and the attenuation of the tissues that are actually in the sound path. Undoing the MI is straightforward. We simply multiply the on-screen number by the square root of the frequency and the attenuation built into the definition of MI. In many cases, this will yield the focal pressure originally measured for the instrument in water.[124–126] We can then apply more realistic attenuations that are applicable to the echocardiographic setting. An idealized transdermal exposure is sketched in Figure 5.

Table 1. Summary of Threshold Data for Lung Hemorrhage

		Lung Hemorrhage Threshold Results					
Nature of Study	Animal	Frequency, MHz	Beamwidth, μm	PRF, kHz	Pulse Duration, μs	Exposure Duration, s	p_r, In Situ, MPa
Threshold[1]	Mouse	2.8	466	1.0	1.4	10	3.6
	Mouse	5.6	448	1.0	1.2	10	3.0
	Rat	2.8	466	1.0	1.4	10	2.3
	Rat	5.6	448	1.0	1.2	10	2.8
Beamwidth[2]	Rat	2.8	470	1.0	1.1	10	3.6
	Rat	2.8	930	1.0	1.1	10	3.5
	Rat	5.6	310	1.0	1.1	10	3.5
	Rat	5.6	510	1.0	1.1	10	3.4
Age dependence[3]	Pig, 5 d	3.1	610	1.0	1.2	10	3.6
	Pig, 39 d	3.1	610	1.0	1.2	10	5.8
	Pig, 58 d	3.1	610	1.0	1.2	10	2.9
Threshold[4]	Rabbit	5.6	510	1.0	1.1	10	3.5
Frequency[5]	Mouse	3.7	NR	0.1	1.0	180	1.4
Threshold[6]	Rat	4.0	NR	1.25	1.0	90	2.0
	Rat	4.0	NR	0.4	1.0	90	2.5
Pulse length[7]	Rat	2.8	470	1.0	1.3	10	3.1
	Rat	2.8	470	1.0	4.4	10	2.8
	Rat	2.8	470	1.0	8.2	10	2.3
	Rat	2.8	470	1.0	11.7	10	2.0
Frequency[8]	Mouse	1.1, U	NR	0.1	10.0	180	0.4
	Mouse	1.2	NR	0.1	10.0	180	0.7
	Mouse	2.3, U	NR	0.1	10.0	180	0.6
	Mouse	3.5, U	NR	0.1	10.0	180	1.3
	Mouse	3.7	NR	0.1	10.0	180	1.0
On time[9]	Mouse	1.2	3500	0.017	10.0	180	1.1
Threshold[10]	Mouse	1.0	1000	0.1	10.0	180	0.4
	Mouse	1.0	1000	1.0	10.0	2.4	1.5
Exposure Duration[11]	Mouse	2.3, U	NR	0.1	10.0	180	0.7
	Mouse	2.3, U	NR	0.1	10.0	20	0.8
Threshold[12]	Pig	2.3	3000	0.1	10.0	120	0.9
Threshold[13]	Pig	2.3	3000	0.1	10.0	120	0.7
Age dependence[14]	Mouse, N	1.15	NR	0.1	10.0	180	0.6
	Mouse, J	1.15	NR	0.1	10.0	180	0.9
	Mouse, A	1.15	NR	0.1	10.0	180	0.7

A indicates adult; J, juvenile; N, neonate; NR, not reported; and U, unfocused transducer.
[1]Zachary et al[109]; [2]O'Brien et al[111]; [3]O'Brien et al[120]; [4]O'Brien et al[117]; [5]Child et al[100]; [6]Holland et al[107]; [7]O'Brien et al[113]; [8]Child et al[100]; [9]Raeman et al[103]; [10]Frizzell et al[92]; [11]Raeman et al[104]; [12]Baggs et al[118]; [13]Dalecki et al[119]; [14]Dalecki et al.[18]

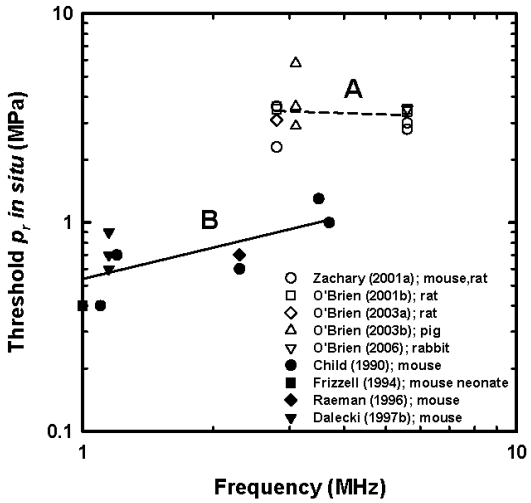

Figure 4. In situ negative pressure thresholds for lung hemorrhage induced by exposure to low–temporal-average intensity pulsed ultrasound in the diagnostic frequency range. Exposures were to mice, rats, and pigs using pulse durations of 1.4 microseconds or less for exposures of 10 seconds (group A) and 10 microseconds for exposures of 180 seconds (group B). Data are culled from Table 1.

Instead of the homogeneous medium envisioned in the definition of MI, the echocardiographic exposure potentially exposes 5 distinctly different tissues, lung, bone, intercostal muscle, heart muscle, and blood, each with its own attenuation characteristics. Lung and bone each have very high attenuation coefficients and acoustic impedances that differ greatly from those of heart muscle and blood. The attenuation of bone is so high that we can exclude any tissue underlying it from consideration. Furthermore, the attenuation of the lung itself is so high that only its superficial tissue is involved in threshold considerations. The attenuation coefficients of the muscle tissues and blood are to a close approximation linear functions of the frequency. Values assumed for these tissues and the attenuation included in the definition of the MI are summarized in Table 2.

For the acoustic pressure p_t in the tissue at the surface of the lung in a diagnostic examination to equal the threshold pressure, the source transducer must be adjusted so that its pressure in water p_w at a corresponding distance from the source is greater than the threshold pressure by the attenuation of the tissues in the path to the lung:

$$p_w = p_t e^{f\sum_i A_i z_i}. \quad (9)$$

A_i and z_i are the attenuation coefficients (normalized to 1 MHz) and path lengths of the tissues in the path, and f is frequency in MHz. To get the desired value of p_w, we would need a screen value of the MI of

$$MI_t = \frac{p_w}{f^{1/2}} e^{-fA_{MI}\sum_i z_i}, \quad (10)$$

or

$$MI_t = \frac{p_t}{f^{1/2}} e^{f(\sum_i A_i z_i - A_{MI}\sum z_i)}. \quad (11)$$

Figure 5. Exposure of lung through the chest wall.

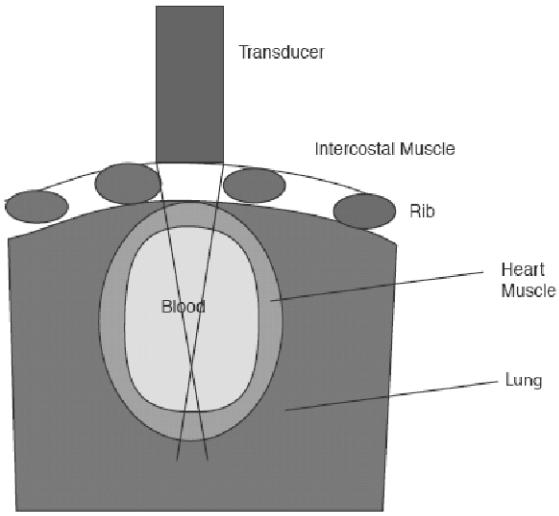

The closest practical window to the heart is through the intercostal tissue. The initial phase of an examination of the heart is spent in a search for the best possible location for the transducer. During that time, lung tissue near the chest wall will be exposed to the near field of the source. Selection of the window automatically eliminates much of the proximal lung simply because it has very high attenuation. While only a very small margin of the beam can hit the lung without seriously limiting the diagnostic information, in many cases, some proximal lung is exposed throughout the examination.

In this case, the actual path is through approximately 2 cm of intercostal tissue instead of the liverlike material assumed in the definition of MI. At 3 MHz, the exponential function in Equation

Table 2. Representative Attenuation Values for Thoracic Tissues

Tissue	Attenuation, Neper/(cm · MHz)	Reference
A_{MI}	0.034	AIUM/NEMA,[124,125] IEC[126]
Intercostal tissue	0.17	Dalecki et al,[18] Baggs et al,[118] Teotico et al,[127] Towa et al,[128] Miller et al[129]
Heart muscle	0.060	O'Donnell et al[130]
Blood	0.024	Carstensen and Schwan[131]

AIUM indicates American Institute of Ultrasound in Medicine; A_{MI}, attenuation included in the definition of the MI; IEC, International Electrotechnical Commission; and NEMA, National Electrical Manufacturers Association.

11 above is 2.3. Referring back to Figure 4, where the thresholds are approximately 1 MPa for the long-pulse exposures (group B) and 3 MPa for the short-pulse exposures (group A), we see that the corresponding values of MI_t are 1.3 and 3.9. Comparing this to the MI limit of 1.9 in most diagnostic devices, we see that damage to the proximal lung can be ruled out in all but atypically long-pulse exposures.

Figure 4 shows that with long pulses, the threshold is approximately 0.6 MPa at 1 MHz. For the case of exposure of the surface of the lung through the intercostal tissue by a transducer in contact with the skin, the MI_t would be 0.8. This example is purely hypothetical, of course. Note that implicit in these computations is the assumption that the focus of the transducer is on the surface of the lung. That would be difficult at frequencies as low as 1 MHz. In fact, it is highly unlikely to occur in any practical echocardiographic examination. In other words, the lung under the ribcage would be exposed to the near field of the transducer. The near field of a focused transducer has many high-pressure regions, but all are significantly lower than the focal pressure. Taking all of these factors into consideration, it appears extremely unlikely that the proximal surface of the lung would be damaged in any normal clinical procedure. The same general considerations allow us to rule out damage to the proximal lung surface in transesophageal examinations.

Consider next lung tissue on the far side of the heart. Although the focus of the sound beam would fall within the heart during most of the examination, it is possible that the focus itself would occasionally fall on the surface of the lung on the distal side of the heart. This worst-case assumption will be used in the calculation. In addition to the attenuation of 2 cm of the chest wall, this path includes roughly 2 cm of heart muscle and 8 cm of blood for a total path of 12 cm. Using this tissue geometry and the attenuation coefficients in Table 2 transforms Figure 4 to Figure 6. Again, for clarity only the extremes of clinically realistic exposures are shown, and the "curve fits" have no great significance but are given simply to assist in evaluating the data.

Figure 6 illustrates that the on-screen values of the MI required to reach the threshold for lung hemorrhage on the distal side of the heart during a transdermal exposure are rather sensitive to the choice of the real tissue path. The solid data points are for the original assumption involving 2 cm each of heart and intercostal muscle and

Figure 6. Threshold data of Figure 4 expressed in terms of on-screen MI for exposures of the lung at the distal surface of the heart (transdermal application). Path 1 includes 2 cm each of intercostal and heart muscle. Path 2 includes 1 cm each of intercostal and heart muscle (see "Lung Hemorrhage, Relating Output to Threshold").

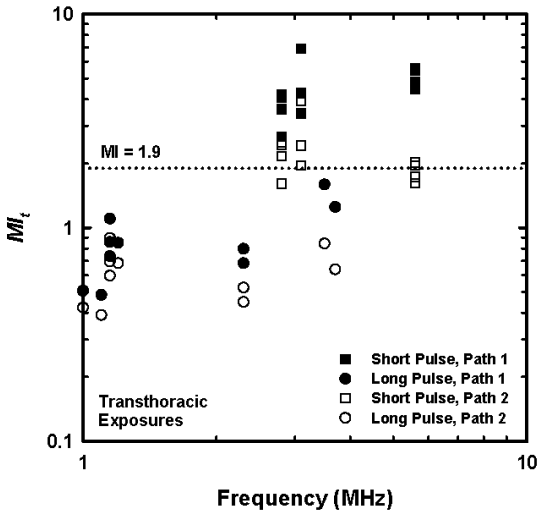

8 cm of blood. The open data points are for the same total distance but with 1 cm each of the muscle tissues replaced by blood.

Because the de facto upper limit for diagnostic ultrasound equipment is an MI of 1.9, Figure 6 shows that lung hemorrhage, in this transducer configuration, is unlikely to occur with the short pulses used in standard B-mode diagnostic examinations, but caution should be exercised with very long pulses and exposure times.

For the lung on the far side of the heart in transesophageal echocardiography, the analysis is the same as it was for the transdermal example except for the absence of the ribcage (ie, 8 cm of blood and 2 cm of heart muscle for a total path length of 10 cm). Here, most of the path has a somewhat lower attenuation than that used in the definition of MI. As a result, it is possible in principle with existing diagnostic machines to produce superthreshold pressures at the lung surface on the distal side of the heart even with the short pulses used in B-mode imaging (Figure 7).

Finally, for an extreme example, consider the following hypothetical scenario. Instead of a specialized short-focus transducer, a pediatric cardiologist uses one with a 10-cm focus with a water-filled standoff. In this case, the only absorber in the path is a 1-cm chest wall. In that case, a 1-MPa threshold at 2 MHz corresponds to an on-screen indication of an MI of 0.5.

Figure 7. Threshold data of Figure 4 expressed in terms of on-screen MI for exposures of the lung at the distal surface of the heart (transesophageal applications).

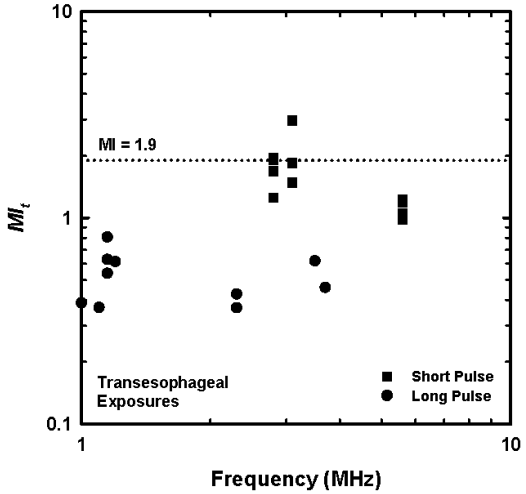

We can conclude the following:

1. There is no single on-screen number that corresponds to the threshold for lung hemorrhage. Each application presents a different problem.
2. We may know outputs with some precision and have a reasonably accurate value for hemorrhage threshold, but relating the two quantities in practical situations involves very large assumptions.
3. As noted below, both positive and negative pressures are equally effective in producing lung hemorrhage. Nonlinear propagation enhances the positive pressure relative to the negative pressure in long-focus sound fields. The MI is defined in terms of the peak negative pressure. There is no simple way to recover the positive pressure in modern systems. However, because a variety of attenuations are involved in possible applications, it is unlikely that any other output indicator could be devised that would be a direct indicator of the threshold for lung hemorrhage.
4. The values used in the examples above are reasonably conservative. From the results, it is clear that lung hemorrhage can occur during realistic diagnostic exposures. Whereas lung hemorrhage is highly unlikely to occur during the bulk of routine diagnostic examinations, to be completely certain that hemorrhage will not occur in all applications would require output levels that compromise the quality of the diagnostic information in many kinds of examinations.

Superthreshold Damage

Because lung hemorrhage is theoretically possible as the result of diagnostic procedures, the nature of the possible damage must be known to balance risk with benefit. The examples above show that even in the focal region of the transducer, it is unlikely that acoustic pressures will greatly exceed the threshold for hemorrhage. In young swine exposed for approximately 4 minutes to 2-MHz focused ultrasound at twice the threshold level (in 10-microsecond pulses with a repetition frequency of 100 Hz), the total area of hemorrhage was approximately 0.3 cm^2.[18] Because of the high attenuation of lung tissue, the region of damage is

confined to a depth of a few millimeters. The most vulnerable tissues are the septa that separate the alveoli. Capillaries there are sufficiently damaged that blood collects in the alveolar space. There is no basis to expect damage in the human lung to be significantly greater than in swine under the same exposure conditions.

The superthreshold lesions that have been observed in experimental animals do not appear to present a clinically significant problem. Even relatively large lesions in rat lung (eg, 30 mm^2) began to resolve within a few days after exposure and by 2 weeks had essentially disappeared, leaving only traces of fibrosis.[109]

Lung hemorrhage in patients will remain hypothetical, supported only by basic biophysical evidence. It is unlikely that damage to the lung would be detected in living subjects if it were to occur.

Mechanism of Lung Hemorrhage

The temporal characteristics of lung hemorrhage make it clear that heating is not a factor in the phenomenon, even taking into consideration the possibility of selective heating at the bone-air structure that surrounds the organ.[132] Instead, the action of ultrasound is purely mechanical.

Even inertial cavitation, which is responsible for many of the biological effects of ultrasound, does not appear to play a significant role in lung hemorrhage. Lung tissue is no more sensitive to ultrasound than other tissues until it fills with air.[133] This appears to have more to do with the fragility of the alveolar walls than to nonlinear oscillation of air bodies. In fact, lung hemorrhage does not appear to have any of the properties that we associate with classical inertial cavitation:

1. The capillaries of the septa, the most sensitive sites for hemorrhage, do not provide an environment conducive to inertial cavitation. In inertial cavitation, the violence of collapse comes from the inertia of inrushing fluid. The environment of the alveolar capillaries, however, is air not liquid.
2. If a few bubbles in the pulmonary capillaries were acting as cavitation sites, adding more bubbles should increase the damage. That is the case for other tissues.[134] However, it does not happen in lung tissue.[114,135]
3. Thresholds for lung hemorrhage are lower than those for hemorrhage in tissues such as intestine[2] and hemolysis in blood and tissues containing exogenous contrast microbubbles[136] where, as discussed below and in the article on contrast agents in this issue,[34] cavitation is more obviously the responsible mechanism. The threshold pressures in Figure 4 and Table 1 are the computed "free-field" pressures at the surface of the lung. Because of the very low impedance of the lung relative to the overlying media, a large fraction of the incident field is reflected and interferes destructively with the incident wave. Probably no more than half of the incident field is transmitted into the lung. It was shown that a deflated lung (having an impedance closer to that of the soft tissue overlying the lung and therefore a higher transmission coefficient) was more easily damaged than an inflated lung.[112,120]
4. Some lung studies show a weak dependence of the threshold on frequency, whereas others[106,109,115] show no significant dependence on frequency. Most of the bioeffects that are clearly related to acoustic cavitation[34] show a stronger frequency dependence.
5. In theory, microbubbles should respond more violently to negative than to positive pressures. That behavior is found in hemorrhage of tissues to which contrast agents have been added.[34,137] In the lung, however, negative pressures cause no greater effect than positive pressures.[116,138]
6. In many applications, it is possible to eliminate inertial cavitation by applying hydrostatic pressures to the medium. The excess pressure acts in two ways: (1) with higher ambient pressures, greater acoustic pressures are necessary to drive the medium into tension; and (2) the application of hydrostatic pressure can drive small bubbles into solution and completely eliminate them as cavitation nuclei. The thresholds for lung hemorrhage are not changed by exposing experimental animals under hyperbaric conditions.[110] Furthermore, the sizes of the lesions were greater under hyperbaric conditions.

None of these observations taken individually clearly rules out inertial cavitation as the mechanism for lung hemorrhage, but taken collectively, the evidence suggests that direct mechanical stresses associated with propagation of ultrasound in the lung are the primary cause of hemorrhage rather than acoustic cavitation. This is supported by the theoretical analysis provided by Fung et al,[139] who modeled the response of a group of gas-filled alveoli to a tensional or compressional wave. The alveoli respond to an incident stress (ie, acoustic pressure) wave by contracting and expanding. During expansion, a tensile stress is generated in the walls of the alveoli, and it is hypothesized that lung trauma is caused by overstretching the alveolar membranes.[140]

Cavitation may become a secondary mechanism of damage once blood begins to pool in the alveoli. Considering the environment, it is possible that this blood would contain microbubbles that would serve as nuclei for inertial cavitation.[103]

Although microbubbles within the lung do not appear to play a significant role in lung hemorrhage, the behavior at audible frequencies of the whole lung acting as a single bubble potentially provides information on the noncavitation damage to the tissues at higher frequencies. The radial oscillation of the adult mouse lung can be modeled by the linear theory of a gas bubble with a resonance frequency of approximately 300 Hz.[141] Exposure of the mouse to that frequency at levels greater than 2 kPa causes extensive hemorrhaging. This is clearly not inertial cavitation. The amplitude of radial oscillation of the lung at the threshold for damage is on the order of 1% of the radius of the lung. The injury does not come from a static stretching of the tissues because normal breathing in the same mode but much below resonance involves somewhat greater amplitudes. Rather, the damage is related to the dynamics of the response of the lung to the sound field. Remarkably, the liver adjacent to the lung, and therefore subject to the same dynamics as the surface of the lung, is hemorrhaged under approximately the same exposure conditions as the lung.

Intestinal Hemorrhage

The intestine appears to be the only organ in the normal body that contains a large concentration of microbubbles that act as ideal nuclei for inertial cavitation. It would be surprising if exposure to ultrasound did not cause damage to the inner wall of the lumen by this mechanism. That this is the case has been shown in several studies performed using both lithotripter pulses[142,143] as well as both pulsed and CW ultrasound at biomedical frequencies.[144–148] Miller and Thomas[145] have shown that heating is the primary mechanism for CW exposures but that a nonthermal mechanism is solely responsible for effects observed with short pulse lengths.

The thresholds for intestinal hemorrhage produced by biomedical ultrasound are shown in Figure 8. It is apparent that the data for hemorrhage in the intestine are rather limited in comparison with those for lung. While the exposure parameters for both the lung and intestine are so diverse that no formal comparison is possible, it is possible to say that thresholds for the intestine tend to be somewhat higher than those for the lung.

Figure 8. Threshold in situ negative pressures for intestinal hemorrhage induced by exposure to low–temporal-average intensity pulsed ultrasound. Pulse lengths were 10 and 100 microseconds at PRFs of 10, 100, and 1000 Hz. Exposures were to mice. Exposure durations were 100 seconds at 400 kHz (▲ and ■), 1000 seconds at 1.09 MHz (○), and 300 seconds at other frequencies (□).

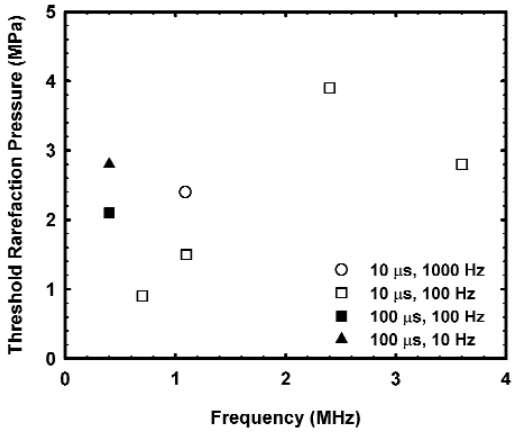

In contrast to the lung, vascular infusion of experimental animals with contrast agents increases the cavitation damage in the intestine.[34,148] In this case, however, the sites of hemorrhage are the capillaries within the intestinal tissue itself rather than within the mucosal-submucosal layer.

Because of the almost random distribution of gas within the intestine, attenuation of the beam passing through the abdomen is highly variable. This creates uncertainty in relating on-screen output information to actual exposure pressures at the focus of the transducer. With this reservation in mind, a reasonable estimate of maximum pressure at the intestine is just the on-screen indication of the MI multiplied by the square root of the frequency.

An Example of Risk Assessment for the Mechanism of Spontaneous Nucleation in Gas-Free Tissue

For the purposes of this document, *risk* is defined as a combination of the probability of occurrence of harm and the severity of that harm, whereas *harm* is defined as physical injury or damage to health.[149] Regarding these two components of risk:

1. *Probability*—Of all of the many nonthermal mechanisms considered here, only one may be considered to have zero probability of occurrence during diagnostic sonography, and even then only at the lowest range of potential outputs. That mechanism is inertial cavitation. It is physically impossible to induce inertial bubble collapse at an output below a well-defined level, even in the presence of bubbles of optimal size. However, these same bubbles will respond to the acoustic field to produce noninertial cavitation; thus, while the probability of inertial cavitation is zero, the probability of harm from all cavitational mechanisms is not zero. Furthermore, while it is true that if no bubbles were present, then the probability would be zero, it is also true that bubbles of any particular size may arise spontaneously due to thermal fluctuations within the tissues of the body. Although the probability of such nucleation events may be vanishingly small, the probability of cavitation of some kind can never be zero.[55,150]
2. *Harm*—There are many nonthermal mechanisms by which ultrasound may affect biological tissue, and some of those interactions may even be sensible to the subject of the examination. While most of these appear to produce no harmful effect on the subject and indeed are not capable of producing harm, at least one type of exposure at diagnostic levels provides a therapeutic benefit: bone healing. It is possible to conceive of a course of events stemming from this effect leading to harm to a patient, but there is no evidence to suggest that this has occurred or is likely ever to occur. Of all the mechanisms considered here, those involving the interaction of ultrasound with gas bodies appear to be the most harmful. Damage to the lung or intestine may occur at gas-tissue interfaces, while inertial cavitation can damage cells and tissues at any point in the body.

From component 1 above, it is reasonable to conclude that the probability of the occurrence of harm is not zero, while from component 2, it is reasonable to conclude that harm may occur during a diagnostic examination. The next step in a determination of risk is to assess the severity of any harm that may occur to the subject. Two limiting cases will be considered here, one common but mild and the other rare but severe.

For the first case, consider petechial hemorrhage in the lung or intestine. Because the in situ threshold rarefactional pressure for an effect is within the diagnostic range, it is reasonable to assume that some patients will have modest damage to their lung during a cardiac examination or to their intestine during an abdominal examination. However, numerous studies have shown that the severity of this damage is very low, and in addition, there is good evidence that such damage heals quickly and completely. Therefore, the risk of permanent harm from exposure to diagnostic ultrasound is extremely small.

For the second case, consider the possibility that isolated inertial cavitation events may transform cells and tissue. While such events are

much rarer than petechial hemorrhage in the lung or intestine, the preceding analysis of the severity of any harm also holds true here.

Two lines of evidence provide an approach to this problem. First, the in vitro results of Doida et al[73,74] show that genetic transformation (ie alteration of one or more genes within viable cells) is achieved with ultrasound only at output levels above the diagnostic range. In contrast, diagnostic levels of x rays produce easily quantifiable levels of transformation in the same cell line (Chinese hamster V-79). Second, Church[55] has quantified the theoretical probability of inertial cavitation events in the absence of exogenous microbubbles in patients under normal conditions (ie, in the absence of conditions recognized to produce artificially high microbubble content in the tissues and vasculature, such as recovery from a rapid decompression from high pressure, or the presence of gas bubble–producing bacterial infections). The results show that the probability of obtaining at most 1 inertial cavitation event during a typical noncontrast ultrasound examination is 1 per 10,000,000,000 examinations, assuming that the acoustic pressure is 4.0 MPa or higher and the MI is 1.8 or higher (the current US Food and Drug Administration limit is MI = 1.9). Combining these results indicates that the probability of cellular transformation from a diagnostic ultrasound examination is very much less (ie, many orders of magnitude less) than is true for a diagnostic x-ray examination. As for the first case considered above, the risk of permanent harm from exposure to diagnostic ultrasound is extremely small.

Summary

Except for the intestine, mammalian tissues, absent exogenous contrast agents, appear to be remarkably free of the small bubbles that may act as cavitation nuclei (note that the lung is a special case in that while it contains a large volume of undissolved gas, this gas is not present in the form of small bubbles). That cavitation nuclei are not completely absent, or may be formed under extraordinary circumstances, is shown by decompression illness and detection of inertial cavitation events after repeated exposure to lithotripter shock waves. The biophysics of inertial cavitation tells us that isolated microbubbles can be activated by diagnostically relevant ultrasound but that the effects of inertial collapse would be highly localized. That is to say, all of the effects that may arise in the presence of contrast microbubbles may in principle also occur in healthy subjects without the introduction of contrast agents but to a much smaller extent. In normal mammalian tissues, the effects are unlikely to be detectable, and the probability of a clinically significant effect at diagnostic levels is very small.

Tissues containing stabilized gas bodies, such as lung, are more susceptible to nonthermal damage by diagnostic ultrasound than are tissues that do not contain undissolved gas. The threshold for adverse effects depends strongly on the in situ acoustic pressure rather than the pressure at the body surface. The dependence on several other parameters (eg, pulse duration and repetition rate, temporal-average intensity, and exposure duration) is relatively weak. The threshold for lung hemorrhage depends on relative inflation, with fully inflated lungs being more resistant to damage. In the biomedical frequency range (>1 MHz), thresholds appear to be only weakly dependent on frequency. Superthreshold exposures produce an extent of nonthermal damage that is strongly dependent on the volume of tissue exposed and the duration of exposure, while the dependence on pulse duration and repetition rate is less. Significantly, there is good evidence that any damage heals quickly and completely. Thus, even if these effects were to occur in some patients, the probability of a clinically significant effect at diagnostic levels is very small.

For other nonthermal biological effects such as bone healing and auditory or tactile sensation, tissues appear to respond not to the (megahertz) carrier frequencies directly but rather to the (kilohertz) PRF of the wave. Regardless of the mechanism, however, none of these effects appear to pose a risk to the health and well-being of the patient undergoing examination by diagnostic ultrasound.

Therefore, it is concluded that the risk of permanent harm from any nonthermal mechanism of action due to exposure to diagnostic ultrasound is extremely small.

Conclusions

1. Tissues containing stabilized gas bodies are more susceptible to nonthermal damage by diagnostic ultrasound than are tissues that do not contain undissolved gas. For these tissues, there are no confirmed reports of adverse biological effects in animals produced by a nonthermal mechanism from exposure to pulsed ultrasound when

$$\frac{p_r}{\sqrt{f}} < 0.4\text{MPa}/\text{MHz}^{1/2},$$

where p_r and f are the in situ values of the rarefactional acoustic pressure and frequency, respectively.
   a. Lung hemorrhage in mouse neonates has been observed after exposure to pulsed ultrasound at in situ peak rarefactional pressures as low as 0.4 MPa at 1.0 MHz for 3-minute exposures to 10-microsecond pulses.
   b. Lung hemorrhage in young pigs has been observed after exposure to pulsed ultrasound at in situ peak rarefactional pressures as low as 1.0 MPa at 2.3 MHz for 2-minute exposures to 10-microsecond pulses.
   c. Lung hemorrhage in adult pigs has been observed after exposure to pulsed ultrasound at in situ peak rarefactional pressures as low as 2.9 MPa at 3.1 MHz for 10-second exposures to 1.3-microsecond pulses. This frequency, pulse duration, and dwell time are characteristic of B-mode imaging.
   d. Intestinal hemorrhage in adult mice has been observed after exposure to pulsed ultrasound at in situ peak-rarefactional pressures as low as 1.5 MPa at 1.1 MHz for 5-minute exposures to 10-microsecond pulses.
2. In tissues that are not known to contain well-defined gas bodies (eg, the spinal cord), there is no evidence of harmful nonthermal biological effects from exposure to 10-microsecond pulses of 1-MHz ultrasound up to a peak rarefactional acoustic pressure of 4 MPa.

Recommendations

Clinical Use

1. Users of diagnostic ultrasound should apply the ALARA (as low as reasonably achievable) principle if the tissues to be exposed contain stabilized gas bodies (eg, lung) and the MI exceeds 0.4.
2. Users should be aware that for soft tissues not known to contain gas bodies, there is no basis in present knowledge to suggest an adverse nonthermal bioeffect from current diagnostic instruments not exceeding the US Food and Drug Administration output limits.

Research (Global)

1. The mechanism by which low-amplitude acoustic fields produce confirmed biological effects, such as accelerated bone healing, should be investigated and, if possible, understood in detail. This information would help to determine whether diagnostic procedures performed at similar levels pose a risk to the patient.

Output Indicators

1. At a given frequency, the MI provides to the clinical user of diagnostic ultrasound a useful but imperfect indicator of risk to the patient. Therefore, use of the MI should be continued, and improvements to the underlying algorithm should be implemented as permitted by better understanding of physical mechanisms and biological effects.
2. Diagnostic ultrasound devices should display the MI if the value of the MI can exceed 0.4; the display should begin at a minimum of 0.1 to allow application of the ALARA principle.

References

1. National Council on Radiation Protection and Measurements. Exposure Criteria for Medical Diagnostic Ultrasound, II: Criteria Based on All Known Mechanisms. Bethesda, MD: National Council on Radiation Protection and Measurements; 2002. Report 140.
2. Dalecki D, Child SZ, Raeman CH, Carstensen EL. Tactile perception of ultrasound. J Acoust Soc Am 1995; 97: 3165–3170.

3. Tsirulnikov EM, Vartanyan IA, Gersuni GV, Rosenblyum AS, Pudov VI, Gavrilov LR. Use of amplitude-modulated focused ultrasound for diagnosis of hearing disorders. Ultrasound Med Biol 1988; 14:277–285.

4. Magee TR, Davies AH. Auditory phenomena during transcranial Doppler insonation of the basilar artery. J Ultrasound Med 1993; 12:747–750.

5. Arulkumaran S, Talbert DG, Nyman M, Westgren M, Hsu TS, Ratman SS. Audible in utero sound from ultrasound scanner [letter]. Lancet 1991; 338:704–705.

6. Fatemi M, Ogburn PL Jr, Greenleaf JF. Fetal stimulation by pulsed diagnostic ultrasound. J Ultrasound Med 2001; 20:883–889.

7. Stratmeyer M, Greenleaf J, Dalecki D, Salvesen K. Fetal ultrasound: mechanical effects. J Ultrasound Med 2008; 27:597–605.

8. Dyson M, Brookes M. Stimulation of bone repair by ultrasound. In: Lerski A, Morley P (eds). Ultrasound '82. Elmsford, NY: Pergamon Press; 1983:61–66.

9. Wang SJ, Lewallen DG, Bolander ME, Chao EYS, Ilstrup DM, Greenleaf JF. Low-intensity ultrasound treatment increases strength in a rat femoral fracture model. J Orthop Res 1994; 12:40–47.

10. Leung K-S, Lee W-S, Tsui H-F, Liu PP-L, Cheung W-H. Complex tibial fracture outcomes following treatment with low-intensity pulsed ultrasound. Ultrasound Med Biol 2004; 30:389–395.

11. Parvizi J, Wu CC, Lewallen DG, Greenleaf JF, Bolander ME. Low-intensity ultrasound stimulates proteoglycan synthesis in rat chondrocytes by increasing aggrecan gene expression. J Orthop Res 1999; 17:488–494.

12. Parvizi J, Parpura JF, Greenleaf JF, Bolander ME. Calcium signaling is necessary for ultrasound-stimulated aggrecan synthesis by rat chondrocytes. J Orthop Res 2002; 20:51–57.

13. Greenleaf JF, Argadine HM, Bolander ME. 1 kHz vibration stimulates ATDC5 chondrocytes. In: Hynynen K (ed). Proceedings of the Fifth International Symposium on Therapeutic Ultrasound. New York, NY: American Institute of Physics; 2006:49–53.

14. Schaden W. Clinical experience with shock wave therapy of pseudarthrosis, delayed fracture healing, and cement-free endoprothesis loosening. In: Siebert W, Buch M (eds). Extracorporeal Shock Waves in Orthopaedics. Heidelberg, Germany: Springer-Verlag; 1997:137–148.

15. Wang C, Chen H, Chen C, Yang K. Treatment of nonunions of long bone fractures with shock waves. Clin Orthop Relat Res 2001; 387:95–101.

16. O'Brien WD Jr, Deng CX, Harris GR, et al. The risk of exposure to diagnostic ultrasound in postnatal subjects: thermal effects. J Ultrasound Med 2008; 27:517–535.

17. Dalecki D, Keller BB, Raeman CH, Carstensen EL. Effects of ultrasound on the frog heart, I: thresholds for changes in cardiac rhythm and aortic pressure. Ultrasound Med Biol 1993; 19:385–390.

18. Dalecki D, Child SZ, Raeman CH, Cox C, Penney DP, Carstensen EL. Age dependence of ultrasonically induced lung hemorrhage in mice. Ultrasound Med Biol 1997; 23:767–776.

19. Purnell EW, Sokollu A, Torchia R, Tanner N. Focal chorioretinitis produced by ultrasound. Invest Ophthalmol 1964; 3:657–664.

20. Lizzi FL, Coleman DJ, Driller J, Franzen LA, Jakobiec FA. Experimental, ultrasonically induced lesions in the retina, choroid, and sclera. Invest Ophthalmol Vis Sci 1978; 17:350–360.

21. Herman BA, Harris GR. Theoretical study of steady-state temperature rise within the eye due to ultrasound insonation. IEEE Trans Ultrason Ferroelectr Freq Control 1999; 46:1566–1574.

22. Nyborg WL. Physical principles of ultrasound. In: Fry FJ (ed). Ultrasound: Its Applications in Medicine and Biology. Part I. New York, NY: Elsevier; 1978:1–75.

23. Nyborg WL. Biological effects of sound and ultrasound. In: Trigg GL (ed). Encyclopedia of Applied Physics. New York, NY: VCH Publishers Inc; 1991:403–420.

24. Dyson M, Woodward B, Pond JB. Flow of red blood cells stopped by ultrasound. Nature 1971; 232:572–573.

25. Nyborg WL. Acoustic streaming due to attenuated plane waves. J Acoust Soc Am 1953; 25:68–75.

26. Stavros AT, Dennis MA. Ultrasound of breast pathology. In: Parker SH, Jobe WE (eds). Percutaneous Breast Biopsy. New York, NY: Raven Press; 1993:111–115.

27. Nightingale KR, Kornguth PJ, Walker WF, McDermott BA, Trahey GE. A novel ultrasonic technique for differentiating cysts from solid lesions: preliminary results in the breast. Ultrasound Med Biol 1995; 21:745–751.

28. Nightingale KR, Kornguth PJ, Trahey GE. The use of acoustic streaming in breast lesion diagnosis: a clinical study. Ultrasound Med Biol 1999; 25:75–87.

29. Trahey GE, Palmeri ML, Bentley RC, Nightingale KR. Acoustic radiation force impulse imaging of the mechanical properties of arteries: in vivo and ex vivo results. Ultrasound Med Biol 2004; 30:1163–1171.

30. Palmeri ML, Frinkley KD, Zhai L, et al. Acoustic radiation force impulse (ARFI) imaging of the gastrointestinal tract. Ultrason Imaging 2005; 27:75–88.

31. Evan AP, McAteer JA, Williams JC, et al. Shock wave physics of lithotripsy: mechanisms of shock wave action and progress toward improved SWL. In: Moore R, Bishoff JT, Loening S, Docimo SG (eds). Textbook of Minimally Invasive Urology. London, England: Martin Dunitz Ltd; 2004:425–438.

32. Howard DD, Sturtevant B. In vitro study of the mechanical effects of shock-wave lithotripsy. Ultrasound Med Biol 1997; 23:1107–1122.

33. Burov VA, Dmitrieva NP, Rudenko OV. Nonthermal impact of high-intensity ultrasound on a malignant tumor. In: Rudenko OV, Sapozhnikov OA (eds). Nonlinear Acoustics at

the Beginning of the 21st Century. Vol I. Moscow, Russia; Moscow State University; 2002:411–416.

34. Miller DL, Averkiou MA, Brayman AA, et al. Bioeffects considerations for diagnostic ultrasound contrast agents. J Ultrasound Med 2008; 27:611–632.

35. Devin C Jr. Survey of thermal, radiation, and viscous damping of pulsating air bubbles in water. J Acoust Soc Am 1959; 31:1654–1667.

36. Leighton TG. The Acoustic Bubble. San Diego, CA: Academic Press; 1994.

37. Prosperetti A. Thermal effects and damping mechanisms in the forced radial oscillations of gas bubbles in liquids. J Acoust Soc Am 1977; 61:17–27.

38. Gilmore FR. The Growth or Collapse of a Spherical Bubble in a Viscous Compressible Liquid. Pasadena, CA: California Institute of Technology; 1952.

39. Flynn HG. Cavitation dynamics, I: a mathematical formulation. J Acoust Soc Am 1975; 57:1379–1396.

40. Keller JB, Miksis MJ. Bubble oscillations of large amplitude. J Acoust Soc Am 1980; 68:628–633.

41. Matsumoto Y, Watanabe M. Nonlinear oscillation of gas bubbles with internal phenomena. Jpn Soc Mech Eng Int J 1989; 32:157–162.

42. Prosperetti A, Lezzi A. Bubble dynamics in a compressible liquid, part 1: first-order theory. J Fluid Mech 1986; 168:457–478.

43. Flynn HG, Church CC. Transient pulsations of small gas bubbles in water. J Acoust Soc Am 1988; 84:985–998.

44. Flynn HG. Cavitation dynamics, II: free pulsations and models for cavitation bubbles. J Acoust Soc Am 1975; 58:1160–1170.

45. Apfel RE. Acoustic cavitation: a possible consequence of biomedical uses of ultrasound. Br J Cancer Suppl 1982; 5:140–146.

46. Apfel RE. Possibility of microcavitation from diagnostic ultrasound. IEEE Trans Ultrason Ferroelectr Freq Control 1986; 32:139–142.

47. Flynn HG. Generation of transient cavities in liquids by microsecond pulses of ultrasound. J Acoust Soc Am 1982; 72:1926–1932.

48. Apfel RE, Holland CK. Gauging the likelihood of cavitation from short-pulse, low-duty cycle diagnostic ultrasound. Ultrasound Med Biol 1991; 17:179–185.

49. Church CC. Frequency, pulse length, and the mechanical index. Acoust Res Lett Online 2005; 6:162–168.

50. Yang X, Church CC. Nonlinear dynamics of gas bubbles in viscoelastic media. Acoust Res Lett Online 2005; 6:151–156.

51. Bailey MR, Pishchalnikov YA, Sapozhnikov OA, et al. Cavitation detection during shock wave lithotripsy. Ultrasound Med Biol 2005; 31:1245–1256.

52. Evan AP, Willis LR, Lingeman J, McAteer J. Renal trauma and the risk of long-term complications in shock wave lithotripsy. Nephron 1998; 78:1–8.

53. Coleman AJ, Kodama T, Choi MJ, Adams T, Saunders JE. The cavitation threshold of human tissue exposed to 0.2-MHz pulsed ultrasound: preliminary measurements based on a study of clinical lithotripsy. Ultrasound Med Biol 1995; 21:405–417.

54. Coleman AJ, Choi MJ, Saunders JE. Detection of acoustic emission from cavitation in tissue during clinical extracorporeal lithotripsy. Ultrasound Med Biol 1996; 22:1079–1087.

55. Church CC. Spontaneous, homogeneous nucleation, inertial cavitation and the safety of diagnostic ultrasound. Ultrasound Med Biol 2002; 28:1349–1364.

56. Miller DL, Thomas RM, Williams AR. Mechanisms for hemolysis by ultrasonic cavitation in the rotating exposure system. Ultrasound Med Biol 1991; 17:171–180.

57. Coakley WT, Nyborg WL. Cavitation, dynamics of gas bubbles: applications. In: Fry FJ (ed). Ultrasound: Its Application in Medicine and Biology. New York, NY: Elsevier; 1978:chap II.

58. Nyborg WL, Miller DL. Biophysical implications of bubble dynamics. In: van Wijngaarden L (ed). The Mechanics and Physics of Bubbles in Liquids. New York, NY: Kluwer; 1982:17–24.

59. Nyborg WL, Miller DL. Biophysical implications of bubble dynamics. Appl Sci Res 1982; 38:17–24.

60. Brayman AA, Miller MW. Cell density dependence of the ultrasonic degassing of fixed erythrocyte suspensions. Ultrasound Med Biol 1993; 19:243–252.

61. Rooney JA. Hemolysis near an ultrasonically pulsating gas bubble. Science 1970; 169:869–871.

62. Rooney JA. Shear as a mechanism for sonically induced biological effects. J Acoust Soc Am 1972; 52:1718–1724.

63. Rooney JA. Hydrodynamic shearing of biological cells. J Biol Phys 1973; 2:26–40.

64. Nyborg WL. Acoustic streaming. In: Hamilton MF, Blackstock DT (eds). Nonlinear Acoustics. San Diego, CA: Academic Press; 1997:chap 7.

65. Cleveland RO, Lifshitz DA, Connors BA, Evan AP, Willis LR, Crum LA. In vivo pressure measurement of lithotripsy shock waves. Ultrasound Med Biol 1998; 24:293–306.

66. Lokhandwalla M, Sturtevant B. Fracture mechanics model of stone comminution in ESWL and implications for tissue damage. Phys Med Biol 2000; 45:1923–1940.

67. Lokhandwalla M, Sturtevant B. Mechanical haemolysis in shock wave lithotripsy (SWL), I: analysis of cell deformation due to SWL flow-fields. Phys Med Biol 2001; 46:413–437.

68. Lokhandwalla M, McAteer JA, Williams JC Jr, Sturtevant B. Mechanical haemolysis in shock wave lithotripsy (SWL), II: In vitro cell lysis due to shear. Phys Med Biol 2001; 46:1245–1264.

69. Makino K, Mossoba MM, Riesz P. Chemical effects of ultrasound on aqueous solutions: evidence for •OH and •H by spin trapping. J Am Chem Soc 1982; 104:3537–3539.

70. Armour EP, Corry PM. Cytotoxic effects of ultrasound: in vitro dependence on gas content, frequency, radical scavengers and attachment. Radiat Res 1982; 89:369–380.

71. Verral RE, Sehgal CM. Sonoluminescence. In: Suslick KS (ed). Ultrasound: Its Chemical, Physical, and Biological Effects. New York, NY: VCH Publishers; 1988:chap 6.

72. Edmonds PD, Sancier KM. Evidence for free radical production by ultrasound cavitation in biological media. Ultrasound Med Biol 1983; 9:635–639.

73. Doida Y, Miller MW, Cox C, Church CC. Confirmation of an ultrasound-induced mutation in two *in-vitro* mammalian cell lines. Ultrasound Med Biol 1990; 16:699–705.

74. Doida Y, Brayman AA, Miller MW. Modest enhancement of ultrasound-induced mutations in V-79 cells *in-vitro* Ultrasound Med Biol 1992; 18:465–469.

75. Coleman AJ, Saunders JE, Crum LA, Dyson M. Acoustic cavitation generated by an extracorporeal shockwave lithotripter. Ultrasound Med Biol 1987; 13:69–76.

76. Kodama T, Takayama K. Dynamic behavior of bubbles during extracorporeal shock-wave lithotripsy. Ultrasound Med Biol 1998; 24:723–738.

77. Delacretaz G, Walsh JT Jr, Asshauer T. Dynamic polariscopic imaging of laser-induced strain in a tissue phantom. Appl Phys Lett 1997; 70:3510–3512.

78. Gracewski SM, Miao H, Dalecki D. Ultrasonic excitation of a bubble near a rigid or deformable sphere: implications for ultrasonically induced hemolysis. J Acoust Soc Am 2005; 117:1440–1447.

79. Zhong P, Zhou Y, Zhu S. Dynamics of bubble oscillation in constrained media and mechanisms of vessel rupture in SWL. Ultrasound Med Biol 2001; 27:119–134.

80. Carstensen EL, Child SZ, Lam S, Miller DL, Nyborg WL. Ultrasonic gas-body activation in *Drosophila*. Ultrasound Med Biol 1983; 9:473–477.

81. Carstensen EL, Campbell DS, Hoffman D, Child SZ, Ayme-Bellegarda EJ. Killing of *Drosophila* larvae by the fields of an electrohydraulic lithotripter. Ultrasound Med Biol 1990; 16:687–698.

82. Barenblatt GI. The mathematical theory of equilibrium cracks in brittle fracture. Adv Appl Mech 1962; 7:55–129.

83. Ortiz M. Microcrack coalescence and macroscopic crack growth initiation in brittle solids. Int J Solids Struct 1988; 24:231–250.

84. Gross DR, Miller DL, Williams AR. A search for ultrasonic cavitation within the canine cardiovascular system. Ultrasound Med Biol 1985; 11:85–97.

85. Ivey JA, Gardner EA, Fowlkes JB, Rubin JM, Carson PL. Acoustic generation of intra-arterial contrast boluses. Ultrasound Med Biol 1995; 21:757–767.

86. Hwang JH, Brayman AA, Reidy MA, Matula TJ, Kimmey MB, Crum LA. Vascular effects induced by combined 1-MHz ultrasound and microbubble contrast agent treatments in vivo. Ultrasound Med Biol 2005; 31:553–564.

87. Fry FJ, Kossoff G, Eggleton RC, Dunn F. Threshold ultrasonic dosages for structural changes in the mammalian brain. J Acoust Soc Am 1970; 48(suppl 2):1413–1417.

88. Dunn F, Fry FJ. Ultrasonic threshold dosages for the mammalian central nervous system. IEEE Trans Biomed Eng 1971; 18:253–256.

89. Frizzell LA. Threshold dosages for damage to mammalian liver by high intensity focused ultrasound. IEEE Trans Ultrason Ferroelectr Freq Control 1988; 35:578–581.

90. Taylor KJW, Pond J. The effects of ultrasound of varying frequencies on rat liver. J Pathol 1970; 100:287–293.

91. Lee CS, Frizzell LA. Exposure levels for ultrasonic cavitation in the mouse neonate. Ultrasound Med Biol 1988; 14:735–742.

92. Frizzell LA, Chen E, Lee C. Effects of pulsed ultrasound on the mouse neonate: hind limb paralysis and lung hemorrhage. Ultrasound Med Biol 1994; 20:53–63.

93. Hynynen K. The threshold for thermally significant cavitation in dog's thigh muscle in vivo. Ultrasound Med Biol 1991; 17:157–169.

94. Fowlkes JB, Parsons JE, Xu Z, et al. The disruption of tissue structure using high-intensity pulsed ultrasound. J Acoust Soc Am 2005; 117:2371.

95. Parsons JE, Cain CA, Fowlkes JB. Characterizing pulsed ultrasound therapy for production of cavitationally induced lesions. In: ter Haar GR, Rivens E (eds). Proceedings of the Fourth International Symposium on Therapeutic Ultrasound. Vol 754. Melville, NY: American Institute of Physics; 2005:178–180.

96. ter Haar GR, Daniels S. Evidence for ultrasonically induced cavitation in vivo. Phys Med Biol 1981; 26:1145–1149.

97. ter Haar GR, Daniels S, Eastaugh KC, Hill CR. Ultrasonically induced cavitation in vivo. Br J Cancer Suppl 1982; 45:151–155.

98. Harvey EN. Physical factors in bubble formation. In: Fulton JF (ed). Decompression Sickness. Philadelphia, PA: WB Saunders Co; 1951:90–114.

99. Buckles RG. The physics of bubble formation and growth. Aerosp Med 1968; 39:1062–1069.

100. Child SZ, Hartman CL, Schery LA, Carstensen EL. Lung damage from exposure to pulsed ultrasound. Ultrasound Med Biol 1990; 16:817–825.

101. Tarantal AF, Canfield DR. Ultrasound-induced lung hemorrhage in the monkey. Ultrasound Med Biol 1994; 20:65–72.

102. Penney DP, Schenk EA, Maltby K, Hartman-Raeman C, Child SZ, Carstensen EL. Morphological effects of pulsed ultrasound in the lung. Ultrasound Med Biol 1993; 19:127–135.

103. Raeman CH, Child SZ, Carstensen EL. Timing of exposures in ultrasonic hemorrhage of murine lung. Ultrasound Med Biol 1993; 19:507–512.

104. Raeman CH, Child SZ, Dalecki D, Cox C, Carstensen EL. Exposure-time dependence of the threshold for ultrasonically induced murine lung hemorrhage. Ultrasound Med Biol 1996; 22:139–141.

105. Zachary JF, O'Brien WD Jr. Lung lesions induced by continuous- and pulsed-wave (diagnostic) ultrasound in mice, rabbits and pigs. Vet Pathol 1995; 32:43–54.

106. O'Brien WD Jr, Frizzell LA, Schaeffer DJ, Zachary JF. Superthreshold behavior of ultrasound-induced lung hemorrhage in adult mice and rats: role of pulse repetition frequency and exposure duration. Ultrasound Med Biol 2001; 27:267–277.

107. Holland CK, Deng CX, Apfel RE, Alderman JL, Fernandez LA, Taylor KJ. Direct evidence of cavitation in vitro from diagnostic ultrasound. Ultrasound Med Biol 1996; 22:917–925.

108. Kramer JM, Waldrop TG, Frizzell LA, Zachary JF, O'Brien WD Jr. Cardiopulmonary function in rats with lung hemorrhage induced by exposure to superthreshold pulsed ultrasound. J Ultrasound Med 2001; 20:1197–1206.

109. Zachary JF, Frizzell LA, Norrell KS, Blue JP, Miller RJ, O'Brien WD Jr. Temporal and spatial evaluation of lesion reparative responses following superthreshold exposure of rat lung to pulsed ultrasound. Ultrasound Med Biol 2001; 27:829–839.

110. O'Brien WD Jr, Frizzell LA, Weigel RM, Zachary JF. Ultrasound-induced lung hemorrhage is not caused by inertial cavitation. J Acoust Soc Am 2000; 108:1290–1297.

111. O'Brien WD Jr, Simpson DG, Frizzell LA, Zachary JF. Superthreshold behavior and threshold estimation of ultrasound-induced lung hemorrhage in adult rats: role of beamwidth. IEEE Trans Ultrason Ferroelectr Freq Control 2001; 48:1695–1705.

112. O'Brien WD Jr, Kramer JM, Waldrop TG, Frizzell LA, Zachary JF. Ultrasound-induced lung hemorrhage: role of acoustic boundary conditions at the pleural surface. J Acoust Soc Am 2002; 111:1102–1109.

113. O'Brien WD Jr, Simpson DG, Frizzell LA, Zachary JF. Threshold estimates and superthreshold behavior of ultrasound-induced lung hemorrhage in adult rats: role of pulse duration. Ultrasound Med Biol 2003; 29:1625–1634.

114. O'Brien WD Jr, Simpson DG, Frizzell LA, Zachary JF. Effect of contrast agent on the incidence and magnitude of ultrasound-induced lung hemorrhage in rats. Echocardiography 2004; 21:417–422.

115. O'Brien WD Jr, Simpson DG, Frizzell LA, Zachary JF. Superthreshold behavior of ultrasound-induced lung hemorrhage in adult rats: role of pulse repetition frequency and exposure duration revisited. J Ultrasound Med 2005; 24:339–348.

116. Frizzell LA, O'Brien WD Jr, Zachary JF. Effect of pulse polarity and energy on ultrasound-induced lung hemorrhage in adult rats. J Acoust Soc Am 2003; 113:2912–2926.

117. O'Brien WD Jr, Yan Y, Simpson DG, et al. Threshold estimation of ultrasound-induced lung hemorrhage in adult rabbits, and comparison of thresholds in rabbits, rats and mice. Ultrasound Med Biol 2006; 32:1793–1804.

118. Baggs R, Penney DP, Cox C, et al. Thresholds for ultrasonically induced lung hemorrhage in neonatal swine. Ultrasound Med Biol 1996; 22:119–128.

119. Dalecki D, Child SZ, Raeman CH, Cox C, Carstensen EL. Ultrasonically induced lung hemorrhage in young swine. Ultrasound Med Biol 1997; 23:777–781.

120. O'Brien WD Jr, Simpson DG, Ho MH, Miller RJ, Frizzell LA, Zachary JF. Superthreshold behavior and threshold estimation of ultrasound-induced lung hemorrhage in pigs: role of age dependency. IEEE Trans Ultrason Ferroelectr Freq Control 2003; 50:153–169.

121. Dalecki D, Raeman CH, Child SZ, Carstensen EL. Lung response to low-frequency underwater sound. J Acoust Soc Am 1999; 106:2165.

122. O'Brien WD, Zachary JF. Mouse lung damage from exposure to 30 kHz ultrasound. Ultrasound Med Biol 1994; 29:287–297.

123. Meltzer RS, Adsumelli R, Risher W, et al. Lack of lung hemorrhage in humans after intraoperative transesophageal echocardiography with ultrasound exposure conditions similar to those causing lung hemorrhage in laboratory animals. J Am Soc Echocardiogr 1998; 11:57–60.

124. American Institute for Ultrasound in Medicine, National Electrical Manufacturers Association. Standard for Real-Time Display of Thermal and Mechanical Indices on Diagnostic Ultrasound Equipment. Laurel, MD: American Institute of Ultrasound in Medicine; Rosslyn, VA: National Electrical Manufacturers Association; 1992.

125. American Institute for Ultrasound in Medicine, National Electrical Manufacturers Association. Standard for Real-Time Display of Thermal and Mechanical Acoustic Output Indices on Diagnostic Ultrasound Equipment. Laurel, MD: American Institute of Ultrasound in Medicine; Rosslyn, VA: National Electrical Manufacturers Association; 1998.

126. International Electrotechnical Commission. Medical Electrical Equipment, Part 2: Particular Requirements for the Safety of Ultrasonic Diagnostic and Monitoring Equipment. Ed 1.1. Geneva, Switzerland: International Electrotechnical Commission; 2004. Publication 60601-2-37.

127. Teotico GA, Miller RJ, Frizzell LA, Zachary JF, O'Brien WD Jr. Attenuation coefficient estimates of mouse and rat chest wall. IEEE Trans Ultrason Ferroelectr Freq Control 2001; 48:593–601.

128. Towa RT, Miller RJ, Frizzell LA, Zachary JF, O'Brien WD Jr. Attenuation coefficient and propagation speed estimates of rat and pig intercostal tissue as a function of temperature. IEEE Trans Ultrason Ferrorelectr Freq Control 2002; 49:1411–1420.

129. Miller RJ, Frizzell LA, Zachary JF, O'Brien WD Jr. Attenuation coefficient and propagation speed estimates of intercostal tissue as a function of pig age. IEEE Trans Ultrason Ferroelectr Freq Control 2002; 49:1421–1429.

130. O'Donnell M, Mimbs JW, Miller JG. The relationship between collagen and ultrasonic attenuation in myocardial tissue. J Acoust Soc Am 1979; 65:512–517.

131. Carstensen EL, Schwan HP. Absorption of sound arising from the presence of intact cells in blood. J Acoust Soc Am 1959; 31:185–189.

132. Hartman CL, Child SZ, Penney DP, Carstensen EL. Ultrasonic heating of lung tissue. J Acoust Soc Am 1992; 91:513–516.

133. Hartman CL, Cox CA, Brewer L, Child SZ, Cox CF, Carstensen EL. Effects of lithotripter fields on development of chick embryos. Ultrasound Med Biol 1990; 16:581–585.

134. Dalecki D, Raeman CH, Child SZ, Penney DP, Mayer R, Carstensen EL. The influence of contrast agents on hemorrhage produced by lithotripter fields. Ultrasound Med Biol 1997; 23:1435–1439.

135. Raeman CH, Dalecki D, Child SZ, Meltzer RS, Carstensen EL. Albunex does not increase the sensitivity of the lung to pulsed ultrasound. Echocardiography 1997; 14:553–558.

136. Dalecki D, Raeman CH, Child SZ, et al. Hemolysis in vivo from exposure to pulsed ultrasound. Ultrasound Med Biol 1997; 23:307–313.

137. Dalecki D, Child SZ, Raeman CH, Xing C, Gracewski S, Carstensen EL. Bioeffects of positive and negative acoustic pressures in mice infused with microbubbles. Ultrasound Med Biol 2000; 26:1327–1332.

138. Bailey MR, Dalecki D, Child SZ, et al. Bioeffects of positive and negative acoustic pressures in vivo. J Acoust Soc Am 1996; 100:3941–3946.

139. Fung YC, Yen RT, Tao ZL, Liu SQ. A hypothesis on the mechanism of trauma of lung tissue subjected to impact load. J Biomech Eng 1988; 110:50–56.

140. Fung YC. Strengh, trauma, and tolerance. In: Biomechanics Motion, Flow, Stress, and Growth. New York, NY: Springer-Verlag; 1990:chap 12.

141. Dalecki D, Child SZ, Raeman CH. Thresholds for sound-induced lung hemorrhage for frequencies from 100 Hz to 1 MHz. J Acoust Soc Am 2006; 119:3375.

142. Raeman CH, Child SZ, Dalecki D, Mayer R, Parker KJ, Carstensen EL. Damage to murine kidney and intestine from exposure to the fields of a piezoelectric lithotripter. Ultrasound Med Biol 1994; 20:589–594.

143. Dalecki D, Raeman CH, Child SZ, Carstensen EL. Thresholds for intestinal hemorrhage in mice exposed to a piezoelectric lithotripter. Ultrasound Med Biol 1995; 21:1239–1246.

144. Lehmann JF, Herrick JF. Biologic reaction to cavitation, a consideration for ultrasonic therapy. Arch Phys Med Rehab 1953; 39:347–356.

145. Miller DL, Thomas RM. Heating as a mechanism for ultrasonically induced petechial hemorrhages in mouse intestine. Ultrasound Med Biol 1994; 20:493–503.

146. Dalecki D, Raeman CH, Child SZ, Carstensen EL. Intestinal hemorrhage from exposure to pulsed ultrasound. Ultrasound Med Biol 1995; 21:1067–1072.

147. Miller DL, Gies RA. The interaction of ultrasonic heating and cavitation in vascular bioeffects on mouse intestine. Ultrasound Med Biol 1998; 24:123–128.

148. Miller DL, Gies RA. Gas-body-based contrast agent enhances vascular bioeffects of 1.09 MHz ultrasound on mouse intestine. Ultrasound Med Biol 1998; 24:1201–1208.

149. International Organization for Standardization. Medical Devices: Application of Risk Management to Medical Devices. Geneva, Switzerland: International Organization for Standardization; 2000. Publication 14971:2000.

150. Herbertz J. Spontaneous cavitation in liquids free of nuclei. In: Fortschritte der Akustik DAGA '88. Bad Honnef, Germany: DPG GmbH; 1988:439–442.